Assessment of Climatic Vulnerability in the Upper Thames River Basin

A report prepared for the Canadian Foundation for Climate and Atmospheric Sciences project:

Quantifying the uncertainty in modelled estimates of future extreme precipitation events

Prepared By:

Leanna King, Tarana Solaiman and Slobodan P. Simonovic, Ph.D., P.Eng.

Department of Civil and Environmental Engineering
The University of Western Ontario
London, ON CANADA N6A 5B9

August 2009

Executive Summary

Increased greenhouse gas emissions are predicted to cause global temperatures to rise in the coming years. It is important to understand and predict the possible impacts of climate change at a local level in order to mitigate these effects and modify the existing infrastructure accordingly. Atmosphere-Ocean General Circulation Models (AOGCM's) are state of the art in climate change assessments. They are essentially predictions of the future climate conditions for grid points around the globe based on plausible emissions scenarios created by the Intergovernmental Panel on Climate Change. The temporal and spatial scales of AOGCM's are very large as they are developed for global impact assessments. Therefore, measures must be taken to provide an estimate of future weather variables on a local scale. Literature is limited on such approaches, and more work is necessary to develop strategies for assessing the impacts of climate change on water resources and communities at both a local and regional level.

This study provides an assessment of possible future climate conditions for the Upper Thames River Basin. Six different AOGCM's with up to three emission scenarios each were used in order to provide a climate change assessment. The data has been scaled down using a principal component analysis integrated stochastic weather generator (WG-PCA) to produce a synthetic dataset of 54 years. The variability between the AOGCM's and their emissions scenarios was investigated, as well as the performance of the WG-PCA generator in producing extreme precipitation events. The results of the study show that the AOGCM results are variable and need to be included when performing future climate change impact assessments in the Upper Thames River Basin. Future work is needed on regional studies to explore local characteristics of precipitation extremes and

improve the model quality by introducing more input variables relevant to the precipitation extremes.

Table of Contents

List of Tables

List of Figures

1. Introduction

One of the most important goals of climate change research is to predict the effects of climate change in order to be prepared for the resulting effects on the natural environment and population. It is a consensus in the scientific community that as the levels of carbon dioxide in the atmosphere rise due to increased greenhouse gas emissions, so will temperatures around the globe. In the recently published 4th Assessment Report of Inter-governmental Panel on Climate Change (IPCC, 2007), it is predicted that the Earth's average temperature is likely to increase by 3^{0}C by 2080 due to the global warming caused by the increased CO_2 emissions. The rising temperature will have a major effect on atmospheric processes, and will likely impact the amount of precipitation a region receives. In climate change impact assessments, precipitation is an important parameter because it is one of the driving factors within the hydrologic cycle. It is of particular importance to look at extremes in precipitation and temperature, as these could have a substantially larger impact on the population than increase in mean temperature alone (Chen et al, 2008). Many studies have indicated that rising global temperature will make these extreme events occur more frequently (Barnett et al, 2006; Wilcox et al, 2007; Allan et al, 2008).

1.1 Background

Water resources are inextricably linked with climate. So the prospect of global climate change has serious implications for water resources and regional development. The 4th Assessment Report by the Intergovernmental Panel on Climate Change (IPCC, 2007) documents the likely impacts on water resources associated with climate change.

Changes in the meteorological variables that drive the hydrologic cycle can be expected to affect the spatial and temporal distribution of water, which can affect the capability of the impacted population to cope with natural hazards related to water excess or shortage.

Assessment of climate change impact on hydrology involves projections of climatic variables at a global scale, downscaling of global scale climatic variables to local scale hydrologic variables and computations of risk of hydrologic extremes in future water resources planning and management (Ghosh, 2007). Increases in extreme rainfall and temperature events are predicted to cause an intensification of the hydrologic cycle in Southwestern Ontario (Prodanovic and Simonovic, 2007). Some effects in particular are changes in stream flows, water supply, and increasing runoff. (Labat et al., 2004; Zhang et al.,2008). Extreme rainfall events are especially important inputs to hydrologic modeling when assessing flood risks in a river basin. Dry spells must also be considered, as low flows and water shortages could become a major problem in the future.

In Canada, warming from 1900 to 2003 has resulted in changes in the climate patterns: (i) a decrease in precipitation as snowfall in the west and the Prairies (Vincent and Mekis, 2006), (ii) a shifting of the magnitude and timing of hydrologic events in regions with winter snow, (iii) earlier spring runoff (Whitfield and Cannon, 2000; Zhang et al, 2001), (iv) an advance of river and lake ice break up by 0.2 to 12.9 days over last 100 years (Magnuson et al., 2000), and so on. Vulnerability to extended drought is increasing across North America as population growth and economic development create more demands from agricultural, municipal and industrial uses, resulting in frequent over-allocation of water resources. Although drought has been more frequent and intense in the western part of Canada, the east is not immune to droughts and reduction in water

supply, change in water quality and ecosystem function, and challenges in water allocation (Wheaton et al., 2005). Hence, it is important to understand and predict the effects of extreme precipitation events in order to modify the existing infrastructure accordingly.

Atmosphere-Ocean General Climate Models (AOGCM's) are developed by various countries around the world and frequently used to predict future changes in the global climate under several plausible emissions scenarios, developed by Inter-governmental Panel of Climate Change (IPCC). Greenhouse gas emissions are used as inputs to AOGCM's from different scenarios, each with a unique storyline based on whether future development is globally or regionally focused, and whether development will be driven by economic or environmental concerns (CCCSN, 2007). AOGCM's discretise the planet into 3 dimensional cells, providing long sequences of gridded climate data that are used for climate change modeling. Unfortunately, cells from current AOGCMs are inappropriate for direct application to the watershed scale because: (i) Accuracy of AOGCMs decreases at finer spatial and temporal scales, a typical resolution of AOGCMs ranges from 250 km to 600 km, but the need for impact studies conversely increases at finer scales; (ii) limited representation of regional topography and (iii) poor representation of mesoscale processes (Eum et al., 2009, Schimidli et al., 2006). Hence, this gridded information must be scaled down to provide information on a local scale relevant to the area being studied, by a process, commonly known as `downscaling`. Different downscaling procedures produce different results from the same AOGCM outputs. So, the downscaled AOGCM outputs are burdened with uncertainties due to intermodal variability (the AOGCM uncertainty), inter-scenario variability (scenario

uncertainty), intermodal variability and variability due to downscaling methods themselves (Ghosh, 2007). The purpose of the study is twofold: to investigate the propagation of AOGCM and inter-scenario uncertainty through climate change modeling and to increase our understanding of the impacts of climate change on extreme precipitation events.

1.2 Organization of the report

This report comprises of several sections: a review of downscaling techniques is presented in section 2. Following this are details on the study area and data used as well as a description of the AOGCM data collected. The WG-PCA weather generator is detailed along with the data preprocessing steps in section 4 of the report. A detailed analysis of the performance of the weather generator and the AOGCM outputs are presented in section 5. Finally, the report concludes with some insights from the results obtained and outlines future work.

2. Literature Review

A number of techniques have been used to generate future climate scenarios. Several authors (Diaz-Nieto and Wilby, 2005; Sharif and Burn, 2006) have used change factor method (also known as Standard Delta method) for generating future times series data. The GCM-simulated difference for each calendar month (absolute difference for temperature and relative difference for precipitation) between a future time period is determined and superimposed in the historic time series to create scenario time series from GCM output.

AOGCMs have been developed to simulate the present climate and used to predict future climate change with forcing by the greenhouse gases and aerosols. These models are not generally designed for local climate change impact studies; thus does not provide satisfactory performance to represent local sub-grid-scale features and dynamics (Wigley et al., 1990; Carter et al., 1994). A number of techniques have been employed to scale down AOGCM outputs to a smaller scale, each with it's own strengths and drawbacks.

Different techniques might be more accurate for different seasons, regions, time periods and depending on the variable being considered (Dibike et al, 2008). The methods include dynamic downscaling that uses complex algorithms at fine-grid scale (typically 50 km x 50 km) describing atmospheric process nested within the AOGCM outputs. (Limited Area Models or Regional Climate Models) and the statistical downscaling which produces future scenarios based on statistical relationship between the larger scale climate features and hydrologic variables. Literatures available for dynamic downscaling include Giorgi (1990, 1992), Walsh and Mcgregor (1995), Druyan

et al (2002), Fowler et al (2005), and so on. The main drawbacks of dynamic downscaling are that the regional climate models require considerable computational resources and cannot meet the need of spatially explicit models of ecosystems or hydrological systems which still requires downscaling the results from such models to individual sites or localities for impact studies (Vidal and Wade, 2008; Wilby and Wigley, 1997). Moreover, re-experiment must be done in case of expanding the region or moving to a slightly different region.

Statistical downscaling, on the other hand, is based on the following assumptions: (i) the predictors are the relevant variables and are realistically modeled by the host AOGCM, (ii) the empirical relationship is also valid for a changed climate and (iii) the predictors adequately represent the climate change signals. Since they are derived from the historic observed data, they can provide site specific information and hence, is recommended in many climate change studies. Dibike et al. (2008), in their comparative study of statistical and dynamic downscaling methods in Northern Canada have found that statistical downscaling represents well the distributions of Tmax and Tmin. The study also reported reduced biases in precipitation with statistical downscaling.

The broad categories of statistical downscaling method include weather generators, weather typing and transfer functions. Weather generators are statistical models of sequences of weather variables which can also be regarded as complex number generators, the output of which resembles daily weather data at a particular location. The parameters of the weather generators are conditioned upon a large scale state, or the relationships between daily weather generator parameters and climatic averages can be used to characterize the nature of future days on the basis of more readily available time

averaged climate change information (Wilks and Wilby. 1999).

Weather generators are important because they allow for more variability in the data, and change the sequencing of wet and dry days. The early work that used weather generators as a downscaling tool in climate change studies can be found in Hughes et al. (1993), Hughes and Guttorp (1994), Hughes et al. (1999) and Wilks and Wilby (1999), etc. An overview of stochastic weather generation models is presented by Wilks and Wilby (1999). The parametric weather generators are associated with several limitations namely: (i) they do not adequately reproduce various aspects of spatial and temporal dependency of variables, (ii) an assumption is necessary regarding the form of probability distribution of variables, which is often, subjective, (iii) non-gaussian features in the data cannot be captured adequately as multivariate autoregressive (MAR) models implicitely assume a normal distribution which is difficult to satisfy, (iv) a large number of parameters are separately fitted to each period and the number further increases if the simulations are to be conditioned, (v) models are not easily transportable to other locations due to the site specific assumptions made regarding the probability distributions of the variables. Non-parametric weather generators can overcome most of these problems and have been used in many studies to produce synthetic datasets. Examples of non-parametric weather generators (WG's) which have been successfully employed in climate change studies are LARS-WG (Semenov and Barrow, 1997), K-NN (Yates et al., 2003; Sharif and Burn, 2006), EARWIG (Kilsby et al, 2007).

Considerable research efforts have been undertaken within the hydrological community to statistically model the high precipitation amount, with a much evidence of it's heavy-tailed distribution (Koutsoyiannis, 2004). But use of weather generators in

improving precipitation extremes is limited. Stochastic weather generators are made to consistently model the precipitation extremes with this information. Furrer and Katz (2008) proposed several possible advanced statistical approaches for improving the treatment of extremes within a parametric GLM based weather generator framework. They found a substantial improvement with a hybrid technique with a gamma distribution for low to moderate intensities and a generalized Pareto distribution for high intensities. Sharif and Burn (2006) used nonparametric K-nearest neighbor weather generator model for simulating extreme precipitation events and found encouraging results in simulating extreme dry and wet spells.

3. Study Area and Data

3.1 Study area

The study area in this report is the Upper Thames River basin, located in Southwestern Ontario, Canada between the great lakes of Erie and Huron. The basin has a population of about 420,000 and covers 3 counties: Perth, Middlesex and Oxford (Figure 1). London, Ontario is the major urban centre with a population of around 350,000. The Thames River is about 273 km long with an average annual discharge of 39.3 m^3/s (Prodanovic, 2008). Thames river basin consists of two major tributaries of the river Thames: the North branch (1,750 km^2), flowing southward through Mitchel, St. Marys, and eventually into London where it meets the South branch; and the South branch (1,360 km^2) flowing through Woodstock, Ingersoll and east London. The basin receives about 1,000 mm of annual precipitation, 60% of which is lost through evaporation and or evapotranspiration, stored in ponds and wetlands, or recharged as

groundwater (Prodanovic and Simonovic, 2006).

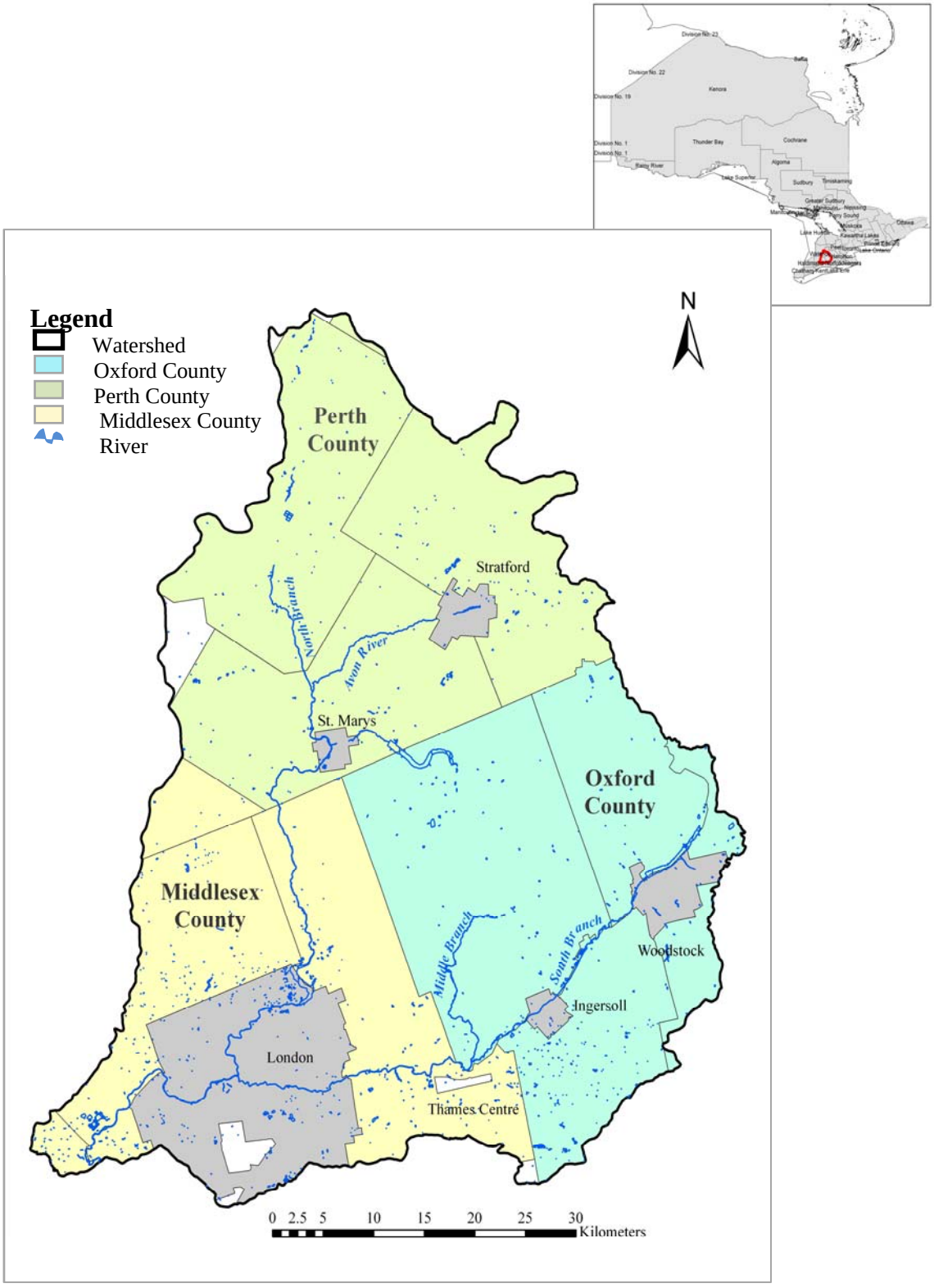

Figure 1: The schematic location map of Upper Thames River basin

The basin often experiences major hydrologic hazards such as floods and droughts. The basin has a well documented history of flooding events dating back to the 1700s. Flooding mostly takes place in early March after the snowmelt and again in July and August as a result of summer storms. Drought conditions also may occur at any time of the year, with highest possibility between June and September. Several weather stations around the basin provide point measurements of weather variables including daily temperature and precipitation. Stations chosen for this study are listed in detail in Table 1 and Figure 2.

Table 1: Location of Stations

Station	**Latitudes (deg N)**	**Longitudes (deg W)**	**Elevation (m)**
Blyth	43.72	81.38	350.5
Brantford MOE	43.13	80.23	196.0
Dorchester	43.00	81.03	271.3
Embro	43.25	80.93	358.1
Exeter	43.35	81.50	262.1
Foldens	43.02	80.78	328.0
Glen Allan	43.68	80.71	404.0
Ilderton	43.05	81.43	266.7
London A	43.03	81.16	278.0
Petrolia Town	42.86	82.17	201.2
Stratford	43.37	81.00	354.0
St. Thomas WPCP	42.78	81.21	209.0
Waterloo_Wellington	43.46	80.38	317.0
Woodstock	43.14	80.77	282.0
Wroxeter	43.86	81.15	355.0

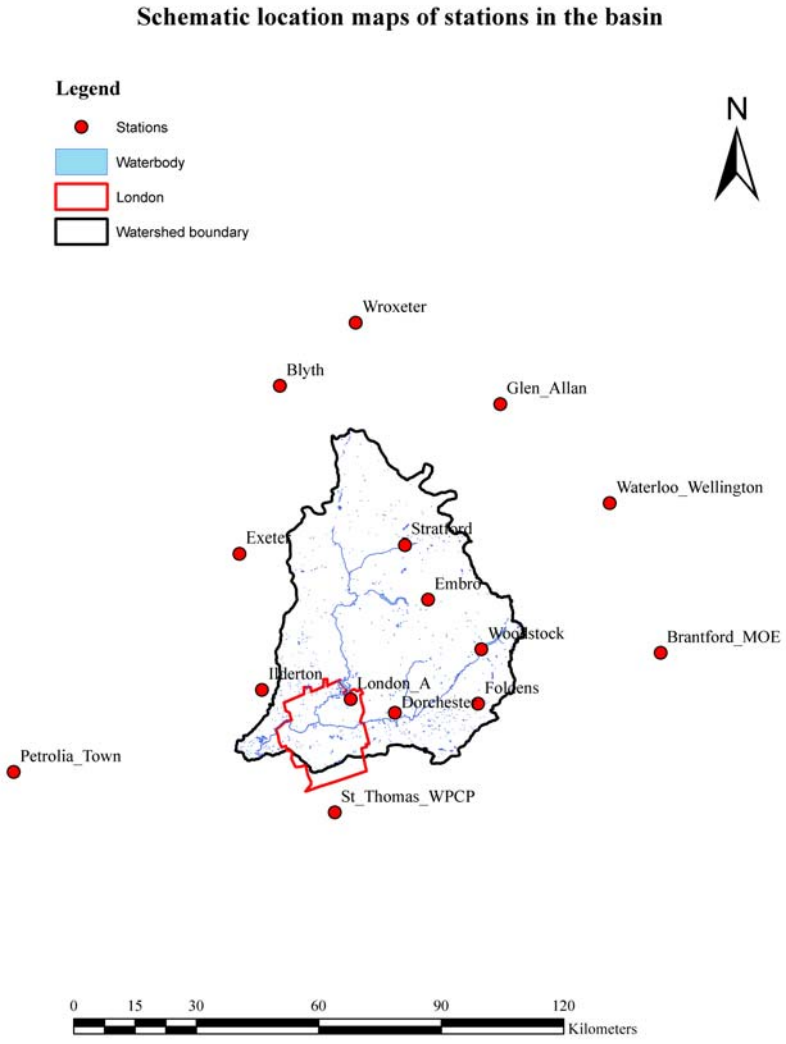

Figure 2: Schematic location map of stations in the basin

3.2 Data

For the purpose of analysis the following databases were used:

- Daily observed precipitation, maximum and minimum temperature (Tmax and Tmin) data covering the UTR basin for the period of 1979-2005 has been collected from Environment Canada (http://climate.weatheroffice.ec.gc.ca/climateData/canada_e.html).

Table 2: List of AOGCM Models and Emissions Scenarios Used

GCM Models	Sponsors, Country	SRES Scenarios	Atmospheric Resolution	
			Lat	Long
CGCM3T47, 2005	Canadian Centre for Climate Modelling and Analysis	A1B, B1, A2	3.75^0	3.75^0
CGCM3T63, 2005		A1B, B1, A2	2.81^0	2.81^0
CSIROMK3.5, 2001	Commonwealth Scientific and Industrial Research Organization (CSIRO) Atmospheric Research, Australia	A1B, A2, B1	1.875 0	1.875 0
GISS-AOM, 2004	National Aeronautics and Space Administration (NASA)/ Goddard Institute for Space Studies (GISS), USA	A1B, B1	3^0	4^0
MIROC 3.2 HIRES, 2004	Center for Climate System Research (University of Tokyo), National Institute for Environmental Studies, and Frontier Research Center for Global Change (JAMSTEC), Japan	A1B, B1	1.125 0	1.125 0
MIROC 3.2 MEDRES, 2004		A1B, A2, B1	2.8^0	2.8^0

- Time series of climate variables for different regions of the world are available at the Canadian Climate Change Scenarios Network (CCCSN) website. These time slices are available for several combinations of AOGCMs and emission scenarios. To obtain weather data for any time slice, the coordinated of the point of interest are specified along with the AOGCM and the emission scenarios. The climate data may be obtained for a number of time slices, each corresponding to future time period. For present study, six AOGCM's climate data for the above variables, each with 2 to 3 emissions scenarios have been collected. The AOGCM's used in the study are the third generation Canadian Coupled Global Climate Model at T47 (CGCM3T47) and T63 (CGCM3T63) resolutions, Australia's Commonwealth Scientific and Industrial Research Organization generated MK3 Climate Systems Model (CSIROMK3.5), Goddard Institute for Space Studies provided Atmosphere Ocean Model (GISS-AOM), the Japanese Model for Interdisciplinary Research on Climate version 3.2 in high (MIROC3.2HIRES) and medium (MIROC3.2MEDRES) resolutions. Three scenarios, A1B, A2 and B1, developed by IPCC's Special Report on Emission Scenarios (SRES) (Appendix A) have

been used in order to investigate the widest possible range of future climates. Table 2 lists the AOGCM's used with the available scenarios for each model.

4. Methodology

4.1 Data preprocessing

Precipitations (PPT), as well as maximum and minimum temperature (Tmax and Tmin, respectively) have been collected from the nearest grid points for each of the six AOGCM's emission scenarios surrounding the Thames River Basin. Data have obtained for two time slices: 1960-1990 and 2041-2070 (2050s).

Preprocessing of the AOGCMs has been carried out in two steps which are explained in the following sections:

4.1.1 Spatial interpolation of AOGCMs

Climate variables from the nearest grid points have been interpolated to provide a dataset for each of the stations of interest. For the purpose of interpolation, the Inverse Distance Weighting Method (IDW) is used. The method works by taking AOGCM variables for the four nearest grid points around the station, and computing the distance from each grid point to the station of interest. A simple formula (4.2.1) is then applied which calculates the weight, *w*, of each grid point based on its distance, *d*, from the station. Next, another formula (4.2.2) computes the value, *p*, for the missing variable (where the subscript *j* represents the j^{th} grid point, and the subscript *i* represents the station of interest).

$$w_1 = \frac{1/d_1^2}{1/d_1^2 + 1/d_2^2 + 1/d_3^2 + 1/d_4^2} \qquad (4.2.1)$$

$$p_i(t) = \sum_{j=1}^{4} w_j p_j(t) \qquad (4.2.2)$$

4.1.2 Calculation of change factors for future climate

Next, a monthly average of each variable is taken for the years 1979-2005 as the base climate and 2041-2070, representative of the future climate in the 2050's. The average monthly differences between the base and future climate have been calculated as the Tmax and Tmin change factors. The percent change in monthly average PPT was calculated, and used as a change factor for precipitation.

The change factors have then, been used to modify the historic dataset which was gathered for each station. Temperature change factors are added to the historic daily temperatures by month, and historic precipitation values were multiplied by the precipitation change factors. Once the historic dataset is modified, it is run through the WG-PCA described above to produce a dataset 54 years long with greater variability for each of the scenarios. A synthetic version of the historic dataset has also been produced to evaluate the performance of WG-PCA.

4.2 Weather generator

Stochastic weather generators simulate weather data to assist in the formulation of water resource management policies. The basic assumption for producing synthetic sequences is that the past would be representative of the future. They are essentially complex random number generators (Eum et al, 2009), which can be used to produce a synthetic series of data with the same statistical properties as the base series. This allows the researcher to account for natural variability when predicting the effects of climate

change. The weather generator used in this study is the refined version of Eum et al (2009), initially developed by Sharif and Burn (2007), which employs integration of Principal Component Analysis in the Weather Generator.

Sharif and Burn (2006) developed an improved K-nearest neighbor weather generator model based on a K-NN resampling strategy proposed by Yates et al. (2003). The K-NN algorithm works by taking one day from the dataset, and selecting a specified number of days which have similar characteristics to that day. One of those days is randomly selected as the weather for the next day using a resampling procedure. In this way, the statistics of the dataset remain the same but the ordering of wet-dry days is changed to add variability to the dataset, which is important in hydrological impact assessments. The major drawback of the K-NN weather generator developed by Yates et al (2003) was that the observed max-min range is the same as that of the synthetic dataset. Sharif and Burn (2007) improved this algorithm by adding a perturbation process that can calculate alternative extremes for the dataset. Their version of K-NN weather generator was further revised by Prodanovic and Simonovic (2006) to account for leap years. Eum et al (2009) further modified the WG to account for more variables.

The WG-PCA algorithm with p variables and q stations has the following steps:

1) Regional means of p variables for all q stations are calculated for each day of the observed data:

$$\overline{X}_t = \lfloor \overline{x}_{1,t}, \overline{x}_{2,t}, \ldots, \overline{x}_{p,t} \rfloor \quad \forall t = \{1,2,\ldots,T\} \qquad (4.1)$$

$$\text{where } \overline{x}_{i,t} = \frac{1}{q}\sum_{j=1}^{q} x_{i,t}^{j} \quad \forall i = \{1,2,\ldots,p\} \qquad (4.2)$$

2) Selection of potential neighbours, L days long where $L=(w+1) \times (N-1)$ for each of p individual variable with N years of historic record, and a temporal window of size w

which can be set by the user of the weather generator. The days within the given window are all potential neighbours to the feature vector. *N* data which correspond to the current day are deleted from the potential neighbours so the value of the current day is not repeated (Eum et al, 2009).

3) Regional means of the potential neighbours are calculated for each day at all *q* stations.

4) A covariance matrix, C_t of size $L \times p$ is computed for day *t*.

5) The first time step value is randomly selected for each of *p* variables from all current day values in the historic record.

6) When more meteorological variables are used in the model, the calculation of Mahalanobis distance becomes challenging due to multi-dimensionality and colinearity associated with the variables. Integration of PCA requires only the variance of the first principal component to calculate the Mahalanobis distance, which reduces the dimension of the mean vector of the current days and the mean vector of all nearest neighbor values. The modified steps are presented here:

(a) Calculation of the eigen vector and eigenvalue for the covariance matrix, (C_t)

(b) Selection of the eigenvector corresponding to the eigenvalue which represents the highest fraction of variance in the *p* variables.

(c) Calculation of the first principle component with equations 4.3 and 4.4 using the eigenvector, *E*, found in (b).

$$PC_t = \overline{X}_t E \qquad (4.3)$$

$$PC_k = \overline{X}_k E \qquad (4.4)$$

where, PC_t is the value of the current day and PC_k is the nearest neighbor transferred

by the eigenvector in (b).

(d) The Mahalanobis distance is calculated with equation 4.5 from the one-dimensional matrix calculated by the above equations.

$$d_k = \sqrt{(PC_t - PC_k)^2 / Var(PC)} \qquad \forall k = \{1,2,...,K\} \qquad (4.5)$$

Where the variance of the first principle component is *Var(PC)* for all *K* nearest neighbors (Eum et al, 2009).

7) The selection of the number of nearest neighbours, *K*, out of *L* potential values using $K = \sqrt{L}$.

8) The Mahalanobis distance d_k is put in order of smallest to largest, and the first *K* neighbors in the sorted list are selected (the K Nearest Neighbors). A discrete probability distribution is used which weights closer neighbors highest in order to resample out of the set of *K* neighbors. Using equations 4.6 and 4.7, the weights, *w*, are calculated for each *k* neighbor.

$$w_k = \frac{1/k}{\sum_{i=1}^{K} 1/i} \qquad \forall k = \{1,2,...,K\} \qquad (4.6)$$

Cumulative probabilities, p_j, are given by:

$$p_j = \sum_{i=1}^{j} w_i \qquad (4.7)$$

9) A random number *u* (0,1) is generated and compared to the cumulative probability calculated above in order to select the current day's nearest neighbor. If $p_1 < u < p_k$, then day *j* for which *u* is closest to p_j is selected. However, if $p_i > u$, then the day which corresponds to *d1* is chosen. If $u=p_K$, then the day which corresponds to day d_K is

selected. Upon selecting the nearest neighbor, the K-NN algorithm chooses the weather of the selected day for all stations in order to preserve spatial correlation in the data (Eum et al, 2009).

10) In order to generate values outside the observed range, perturbation is used. A conditional standard deviation, σ, is estimated and using equation 4.8 a bandwidth, λ,is determined.

$$\lambda = 1.06\sigma K^{1/5} \qquad (4.8)$$

Perturbation is next, using equation 4.9.

$$y_{i,t}^{j} = x_{i,t}^{j} + \lambda\sigma_{i}^{j} z_{t} \qquad (4.9)$$

Where $x_{i,t}^{j}$ is the weather variable obtained in step 9, $y_{i,t}^{j}$ is the value of that variable obtained after perturbation, z_t is a random variable which is normally distributed (zero mean, unit variance) for day *t*. Negative values are prevented from being produced for precipitation by employing a largest acceptable bandwidth: $\lambda_a = x_{*,t}^{j} / 1.55\sigma_{*}^{j}$ where * refers to precipitation. If again a negative value is returned, a new value for z_t is generated (Sharif and Burn, 2006).

5. Results and Discussion

This study uses daily precipitation, maximum temperature and minimum temperature of 15 stations for the period of 1979-2005 (N=27) to simulate plausible meteorological scenarios. Employing the temporal window of 14 days (w=14) and 27 years of historic data (N=27), this study uses 404 days as the potential neighbors *(L=(w+1) x N-1=404)* for each variable. The study has generated synthetic meteorological scenarios which is

equal to the historic data in length in order to allow for the statistical comparison of synthetic and historic data. For the purpose of comparing performances of AOGCM's WG results for London station has been chosen. The following sections present the analysis of the obtained results in reproducing present and future climate.

5.1 Reproduction of historic data

Using the WG-PCA weather generator of Eum et al (2009), 54 years of synthetic data are produced using the historic dataset in order to determine if the WG-PCA algorithm has been able to produce a dataset with statistically similar characteristics to the observed values. Box plots have been used to illustrate the results, as they provide a wide range of variation of the dataset's statistics. The top and bottom lines of the plot represent the 75^{th} and the 25^{th} percentiles, respectively. The middle line in the box represents the median. The whiskers extend out to 1.5 times the inter-quartile range of the data (range of the data between the 25^{th} and 75^{th} percentiles). Values that go beyond those points, have been identified as outliers and marked in black.

Figure 3 consists of monthly box plots of the 54 simulated years of data for maximum temperature in London, as well as a line plot illustrating the means of the observed data. Despite the weather generator being applied to daily data, the box plots have been made on a monthly scale in order to facilitate presentation of the results. The WG-PCA simulated results are clearly able to reproduce the historic monthly values, despite the fact that the algorithm has been applied on a daily scale. The output of the weather generator in reproducing temperature values is highly satisfactory.

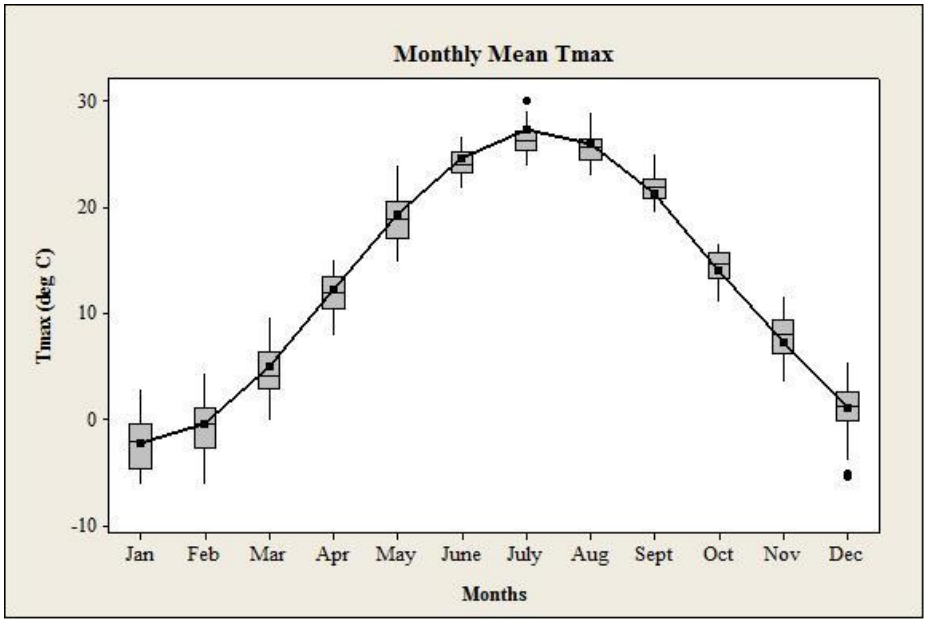

Figure 3: Box plots of monthly mean maximum temperature

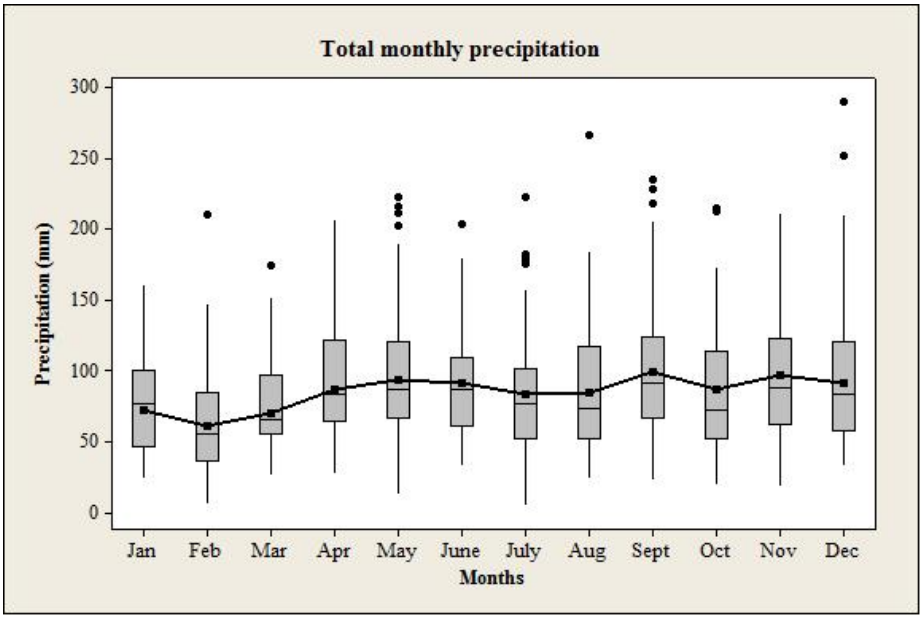

Figure 4: Box plots of total monthly precipitation

Total monthly precipitation values for the simulated data are presented as box plots in Figure 4. The historic mean values are represented by the line plot. For all of the months, the median of the simulated data is close to the mean of the observed data. There

is a slight underestimation in total precipitation for the months of August, September, October, November and December. For the rest of the months, the mean total precipitation of the observed data is very close to the median of the simulated data. There are a number of outliers, marked as black dots; however these are representative of the increased variability due to the perturbation process in the weather generator. Precipitation has the greatest variability of all the weather variables, so overall the performance of the WG-PCA algorithm in this aspect is very good.

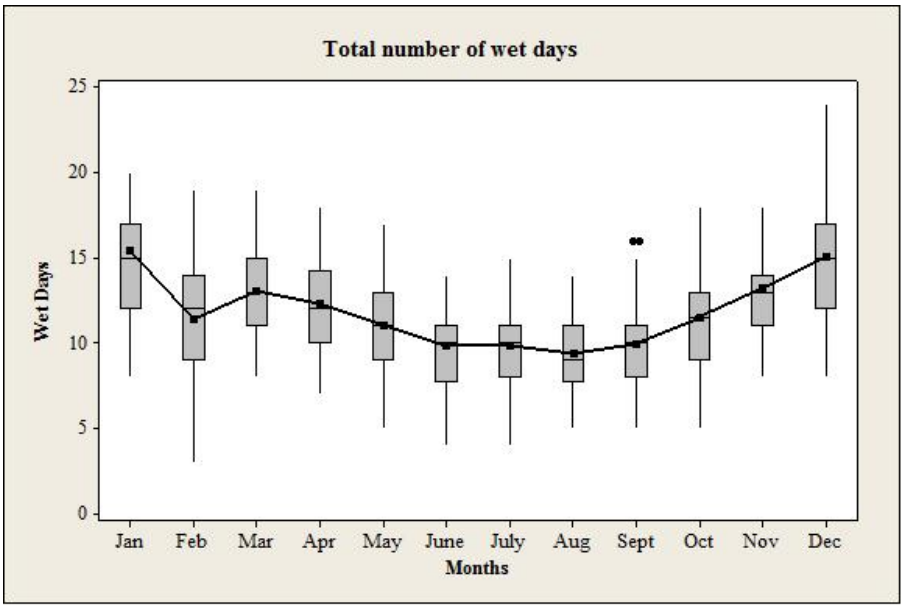

Figure 5: Box plots of total number of wet days

The number of wet days for the simulated data in London is illustrated as monthly box plot in Figure 5. Wet day statistics are very important when it comes to hydrologic modeling and flood management. The observed means are shown as a line plot. It is clear that the observed values agree very well with the simulated data. There is a slight overestimation by the simulated data for the month of February and an underestimation for January but the results are otherwise very good.

5.2 Correlation Structure

It is important to preserve the correlation structure of the observed data intact in the simulated data. To keep the inherent correlation structure unaltered, the modified versions by Sharif and Burn (2007) and Eum et al. (2009) used a constant value of the random normal variate for all the variables and all stations at any given time step. This section investigates the extent to which the correlation structure changed from the observations. Figure 6 presents box plots of the monthly correlations between precipitation and maximum temperature. Observed data has shown positive correlation during winter months; correlations during summer months are very close to zero which indicates a statistically insignificant correlation for these months.

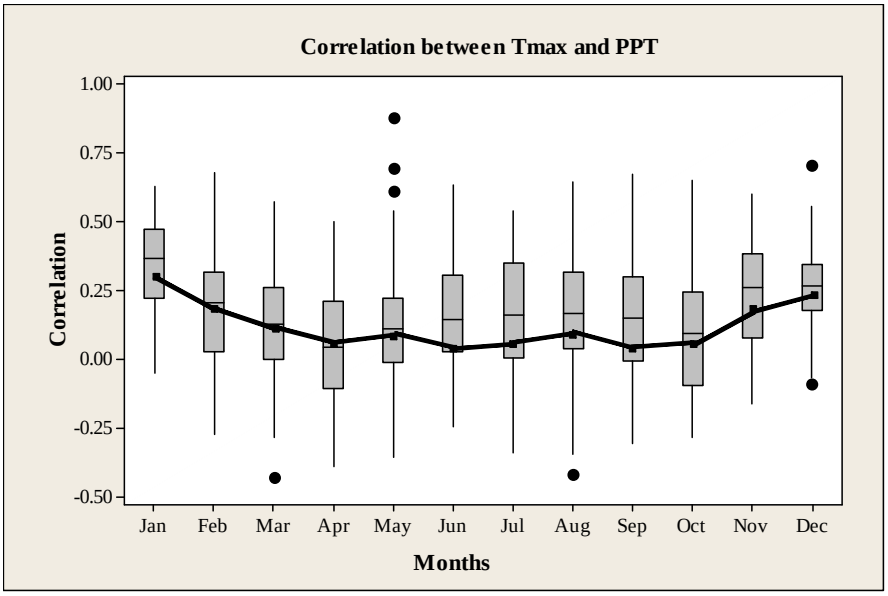

Figure 6: Box plots of correlation between Tmax and PPT

5.3 Generation of climate change scenario

Major focus of this study is to evaluate the performance of WG-PCA in simulating the future precipitation amounts which may be larger than the observations. This section

presents the performances of WG-PCA in simulating 54 year's of future precipitation using the informations from the AOGCM's with plausible scenarios.

First, bar graphs have been used to illustrate the change factors for the various AOGCM's and emissions scenarios. Figure 7 shows the monthly change factors for Tmin. All models predict an increase in the minimum temperature,ranging from 1.5^0 C to 6^0 C; the magnitude of increase is however, diffierent for different models. For example, in the month of February, there is a difference of 4.8°C in the predicted temperature changes of CGCM3T63 scenario A1B and GISS-AOM scenario B1. The variation of the change fields are more prominent during winter months. The MIROC-HIRES model for A1B and B1 scenarios have shown consistent increase of Tmins all through the year ranging between 3-4^0C. The CGCM3T63 has shown lager variability in different months of the year, predicting an increase ranging from 1.5 to 6^0C for scenarios A1B and A2. For the summer months, the predictions match quite well with variability less than 1^0C except for MIROC-HIRES and MEDRES models. The monthly Tmax change factors for all models are shown in Figure 8. Again, the variability between the models and scenarios can be clearly seen from the graph. A substantial difference is seen for the winter months of January, February, March and in late summer months. The greatest difference has been found for the month of March; there has been a difference of over 5.1°C between the predicted change fields for MIROC3.2MEDRES scenario A1B and GISS-AOM scenario B1. All other months had a range of at least 1.4°C between the lowest and highest predicted temperature change.

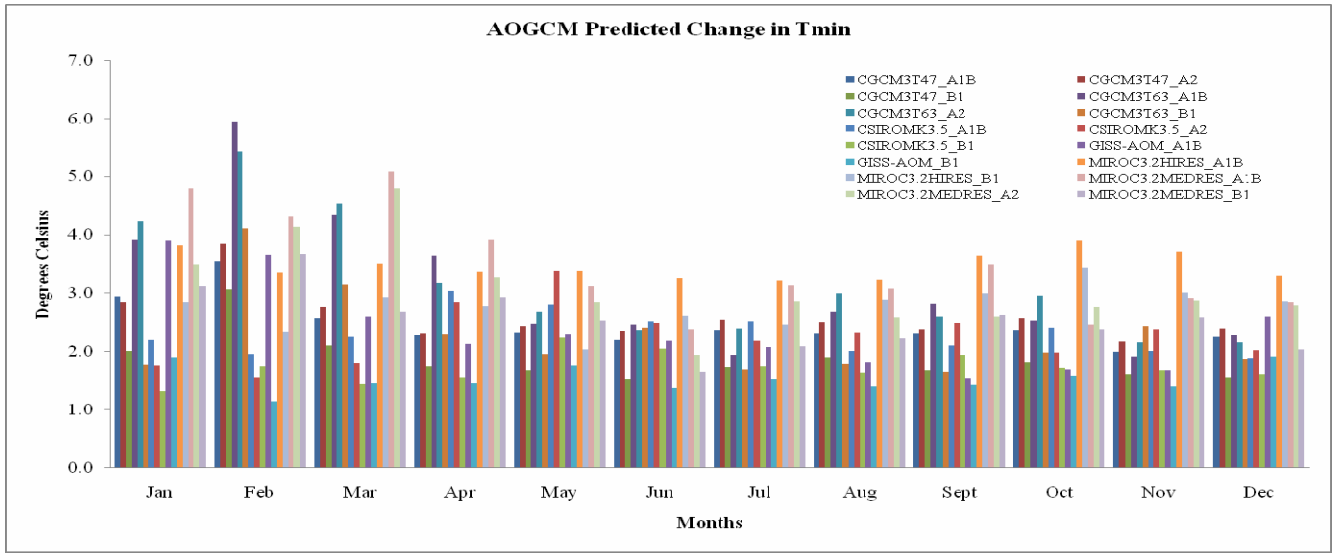

Figure 7: AOGCM predicted change factors for minimum temperature

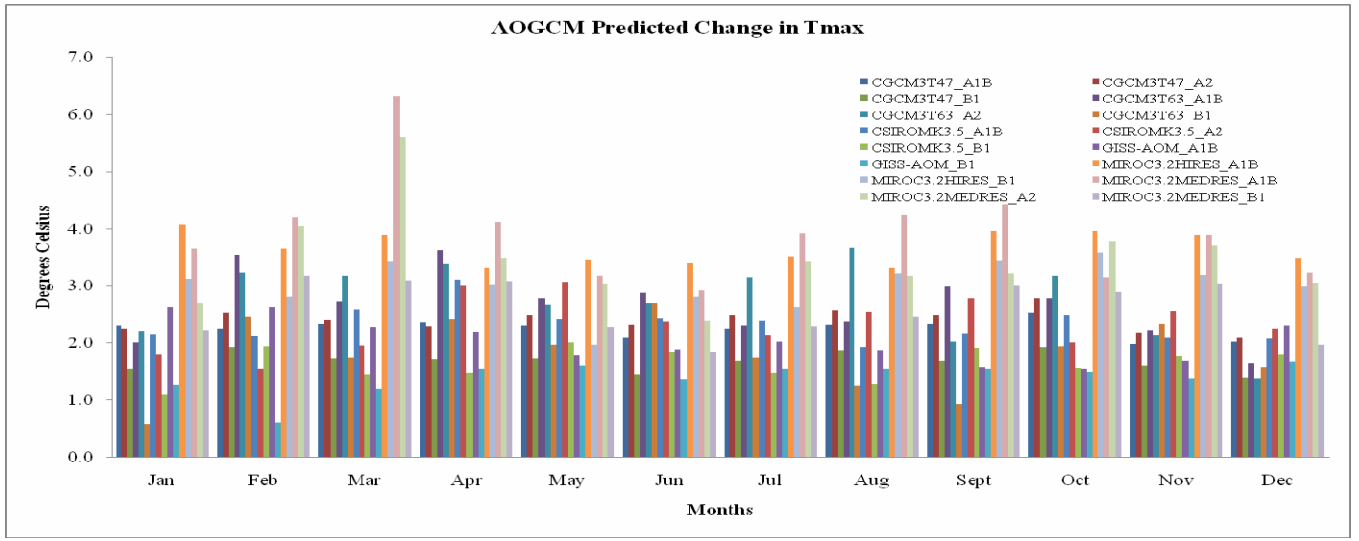

Figure 8: AOGCM predicted change factors for maximum temperature

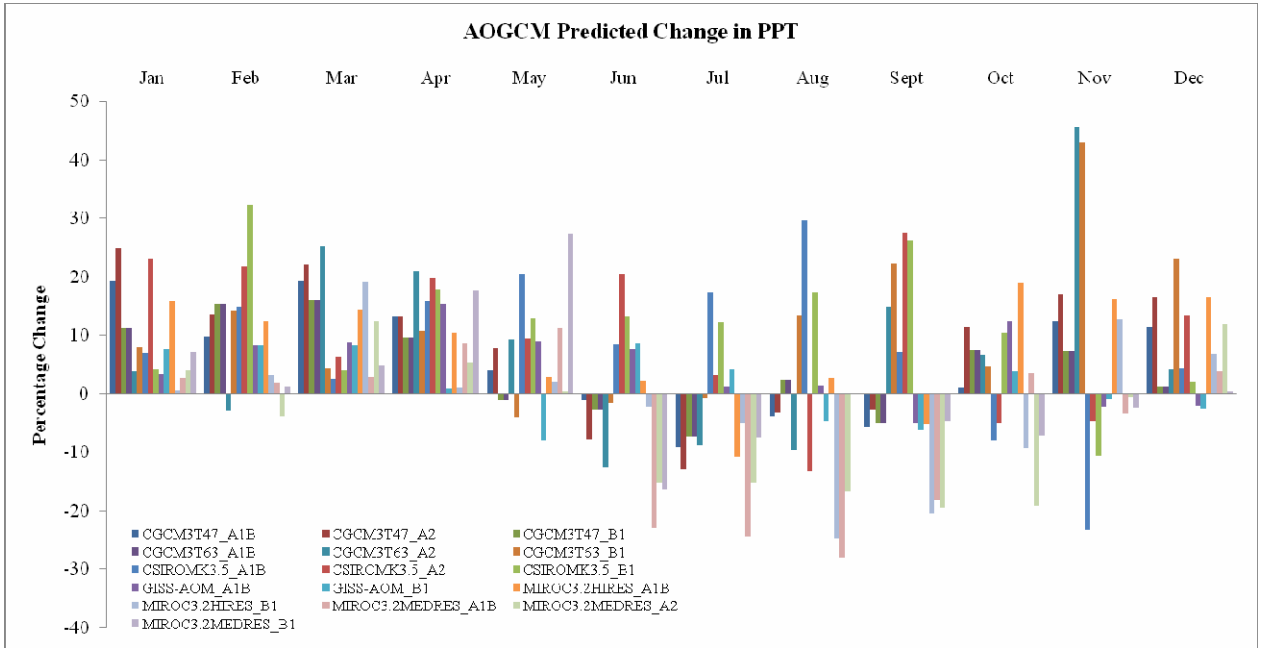

Figure 9: AOGCM predicted percent changes in precipitation

The change factors for precipitation are illustrated as percentage changes in Figure 9. The differences in projections are largest in case of precipitations as compared to Tmax and Tmins. While one scenario has predicted an increase, other may have associated with a decrease in precipitation for any specific month. This is more evident during the summer months of May to November. For example, during November, the difference between CGCM3T63 scenario A2 and CSIROMK3.5 scenario A1B is 68.9 percent.Despite wide variations in predictions, one interesting observation is that all scenarios have predicted increase in winter precipitation from December through April. The wide range of different future climate projections in Figures 8 through 10, thus clearly suggests to interprete the obtained results as plausible scenarios rather than as predictions of future climate conditions.

Next, line plots (Figures 10 through 12) are from the simulated weather data conditioned to the plausible climate change sceanrios derived from several scenarios.. Figures marked (a) consist of all emissions scenarios for the models CGCM3T47, CGCM3T63, and GISS-AOM. Figures marked (b) consist of all scenarios for the models CSIROMK3.5, MIROC3.2MEDRES, and MIROC3.2HIRES. Figures 10 a and shows the AOGCM predicted total monthly precipitation values of the simulated data, along with the historic simulated data as a reference. While the overall shapes of the plots are similar, it is clear that there is a wide range of variability in the AOGCM predictions. For the months of February and March, most AOGCM simulations predict an increase in precipitaiton, but the range of increase between the lowest and highest is quite large, almost 30 mm. All models but two (CGCM3T63 B1 and MIROC3.2 HIRES B1) predict an increase in the average precipitation in April. For most other months, some simulations predict an increase where others predict a decrease.

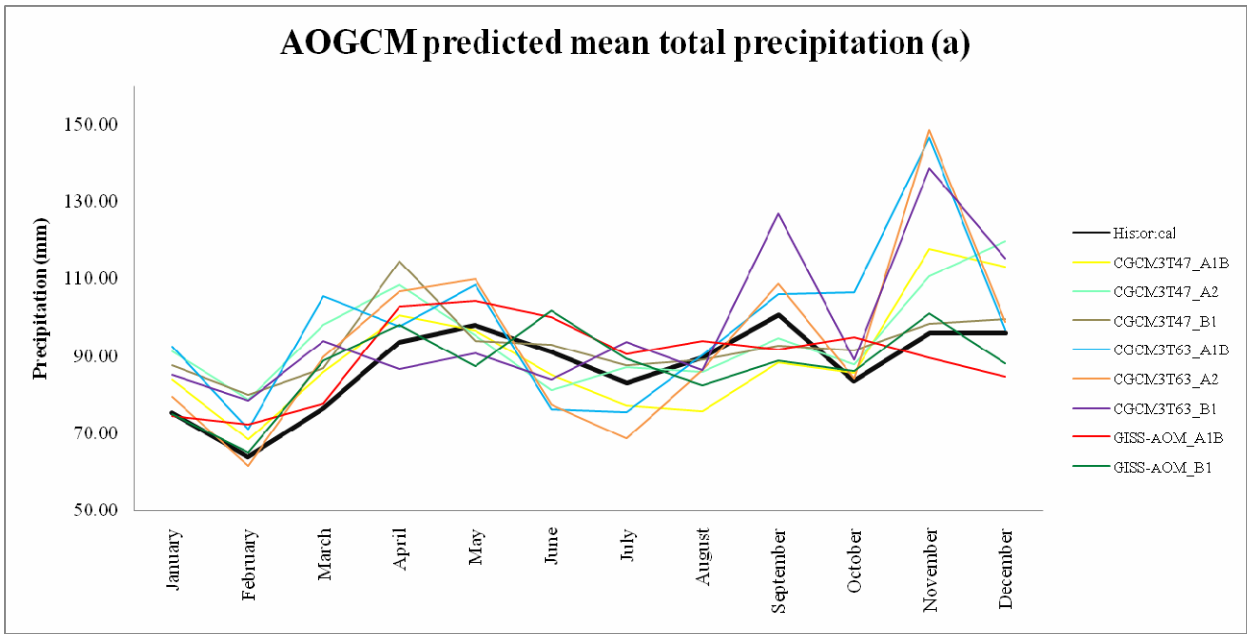

Figure 10a: AOGCM predicted average total precipitation compared with historical averages

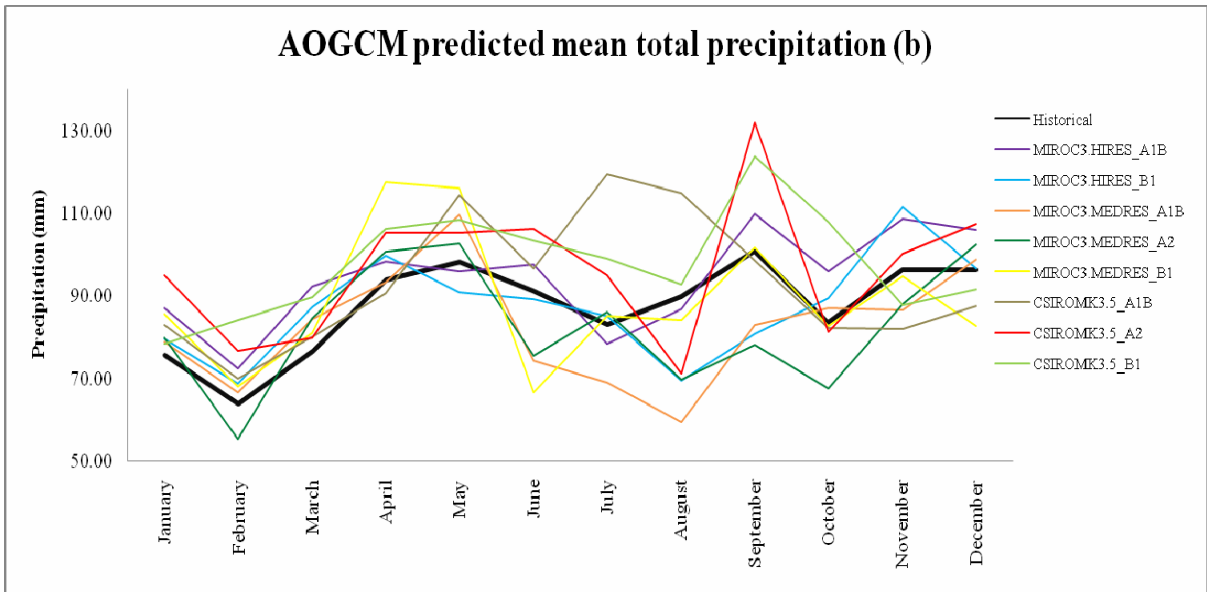

Figure 10b: AOGCM predicted average total precipitation compared with historical averages

Predictions for AOGCM maximum temperatures are shown in Figures 11a and 11b. All simulations predict an increase in the the maximum temperature for all months. The amount of increase differs with each model, as discussed in the change factor bar graphs in Figure 8. MIROC3.2MEDRES scenario A1B predicts an average maximum temperature of 10.5°C for March (Figure 11b), while GISS-AOM scenario B1 predicts a March average of 5.5°C (Figure 11a). Since snowmelt is a major flooding risk in the basin, this difference would have a significant impact of the timing and magnitude of peak runoff.

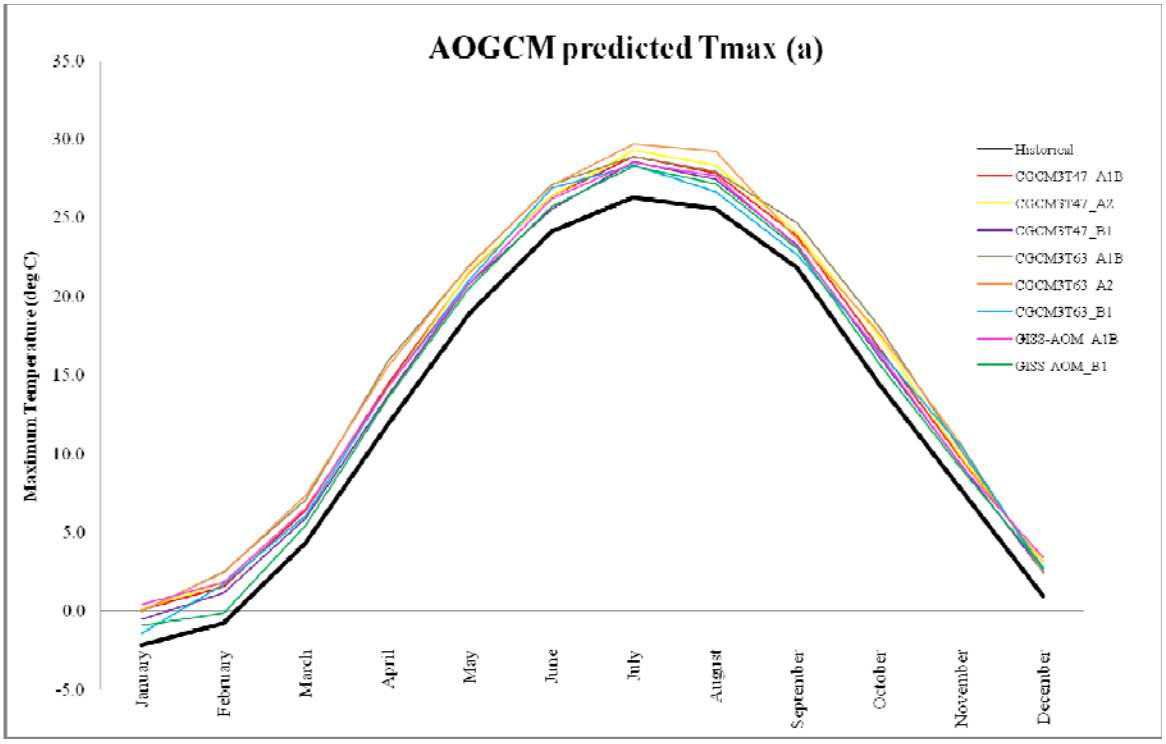

Figure 11a: AOGCM predicted average monthly maximum temperatures compared to historical averages

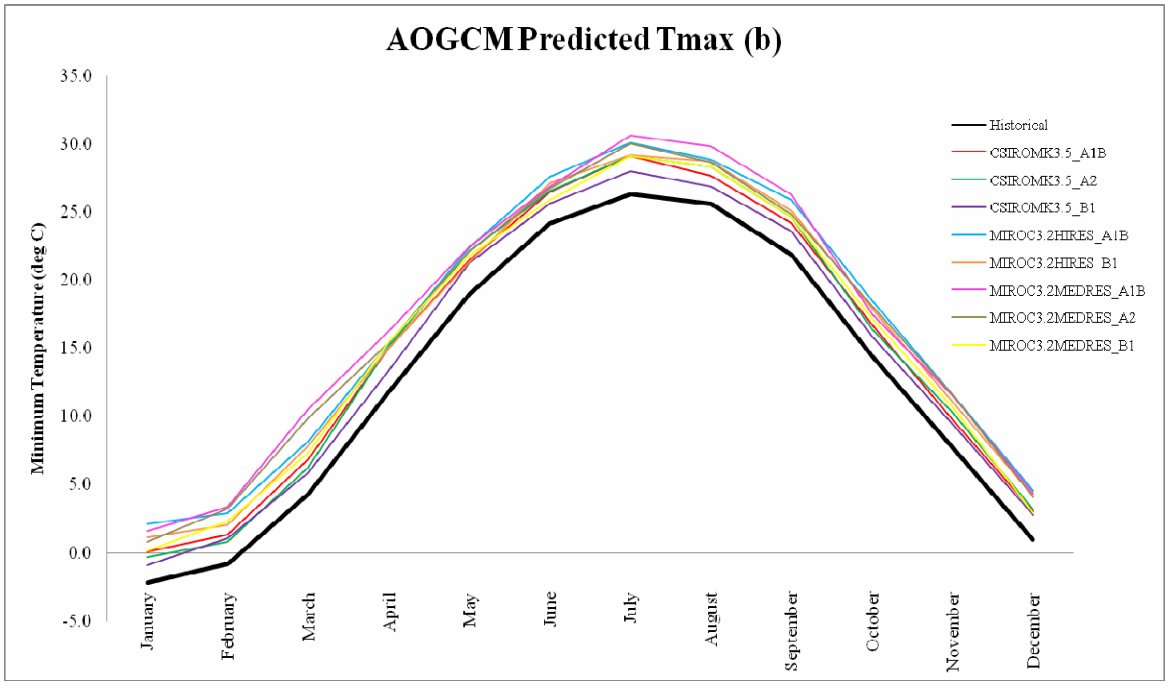

Figure 11b: AOGCM predicted average monthly maximum temperatures compared to historical averages

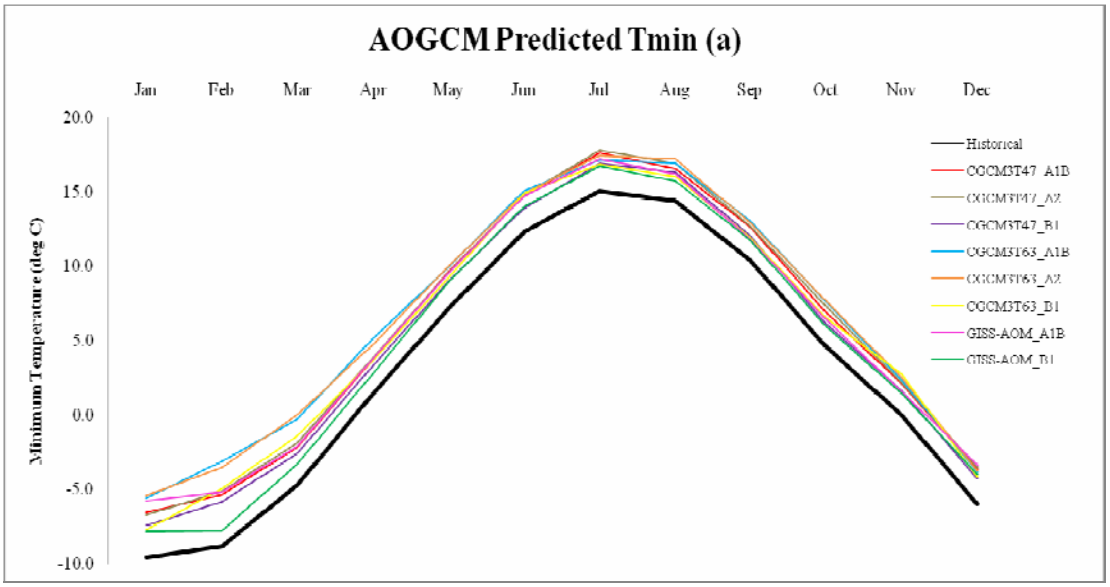

Figure 12a: AOGCM predicted average monthly minimum temperature compared with historical averages

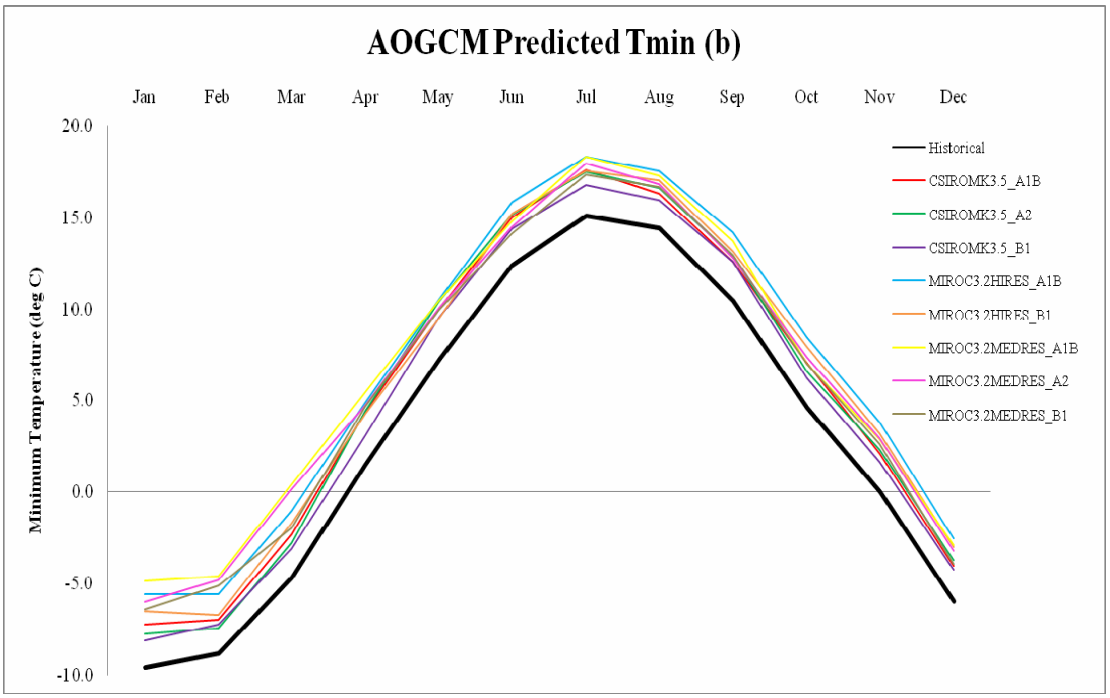

Figure 12 b: AOGCM predicted average monthly minimum temperature compared with historical averages

Minimum temperature predictions are illustrated in Figures 12a and b. For all

months, the simulations predict an increase in the average monthly minimum temperature. It is clear that the magnitude of this increase for the simulations is variable. For the month of February, there is the most variability in the predictions. For example CGCM3T63 scenario A1B predicts a minimum temperature of -3.1°C, while the model GISS-AOM scenario B1 predicts an average minimum temperature of -7.8°C. The AOGCM predictions for the month of May display the least variability. MIROC3.2MEDRES scenario A1B has a minimum temperature for May of 10.4°C, which is relatively close to the 8.9°C prediction of simulation GISS-AOM scenario B1.

Box plots of total monthly mean precipitation for all scenarios are presented in box plots 13 through 18. Figure 13 shows the box plots for the model CGCM3T47 scenarios A1B, A2 and B1, respectively. It is clear by the number of outliers that the WG-PCA weather generator has been able to produce a dataset adequately. For summer month, especially from May through September, A1B and B1 scenarios have predicted a decrease in precipitation while A2 has predicted less precipitation for June and August. The precipitation generated for the month of November in A2 scenario is the only month where the observed precipitation falls below the 25^{th} percentile value of A2.

The monthly precipitation box plots for the CGCM3T63 model are illustrated in Figure 14. Overall, the months of November and September have the greatest range of monthly precipitation totals among all of the emissions scenarios. The medians for November were the highest in all scenarios. The inter-quartile ranges (the boxes) of SRES scenario A1B were much larger than those of A2 and B1. Unlike CGCM3T47 model, A1B and B1 scenarios of CGCM3T63 have projected a decrease in precipitation only in two summer month: June and July by A1B and May and June by B1. However

CGCM3T63 A2 has projected wider variability: a decrease in precipitation during most of summer and increase of precipitation during winter. Overall, the performance of the model in producing the changes in monthly precipitation totals has proved satisfactory only except for November.

The precipitation produced by CSIROMK3.5 is different than the CGCM models (Figure 15). All months but September, October, and November has projected decrease in precipitation. A similar trend has been seen for the GISS-AOM A1B and B1 scenario simulations (Figure 16). SRES Scenario A1B predicts increase of early springtime precipitation and extended period of summer precipitation with greater variability than scenario B1. The high resolution MIROC3.2 model has predicted decrease of precipitation in all months except December, January, February and March (Figure 17). A similar trend is seen for the mid resolution MIROC3.2 A1B and B1 too (Figure 18).

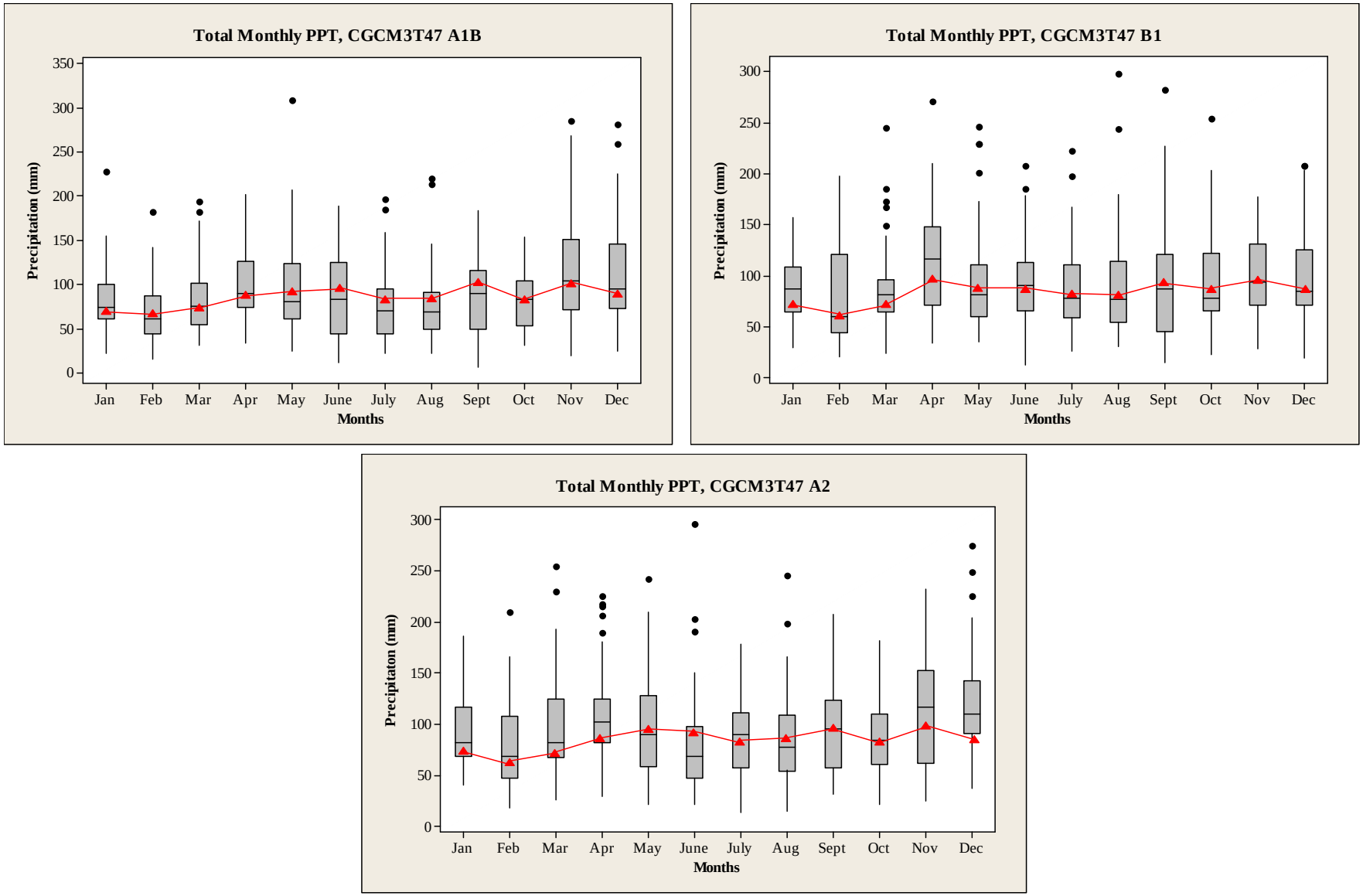

Figure 13: Box plots of CGCM3T47 generated monthly precipitation for A1B (upper left), A2 (upper right) and B1 scenarios

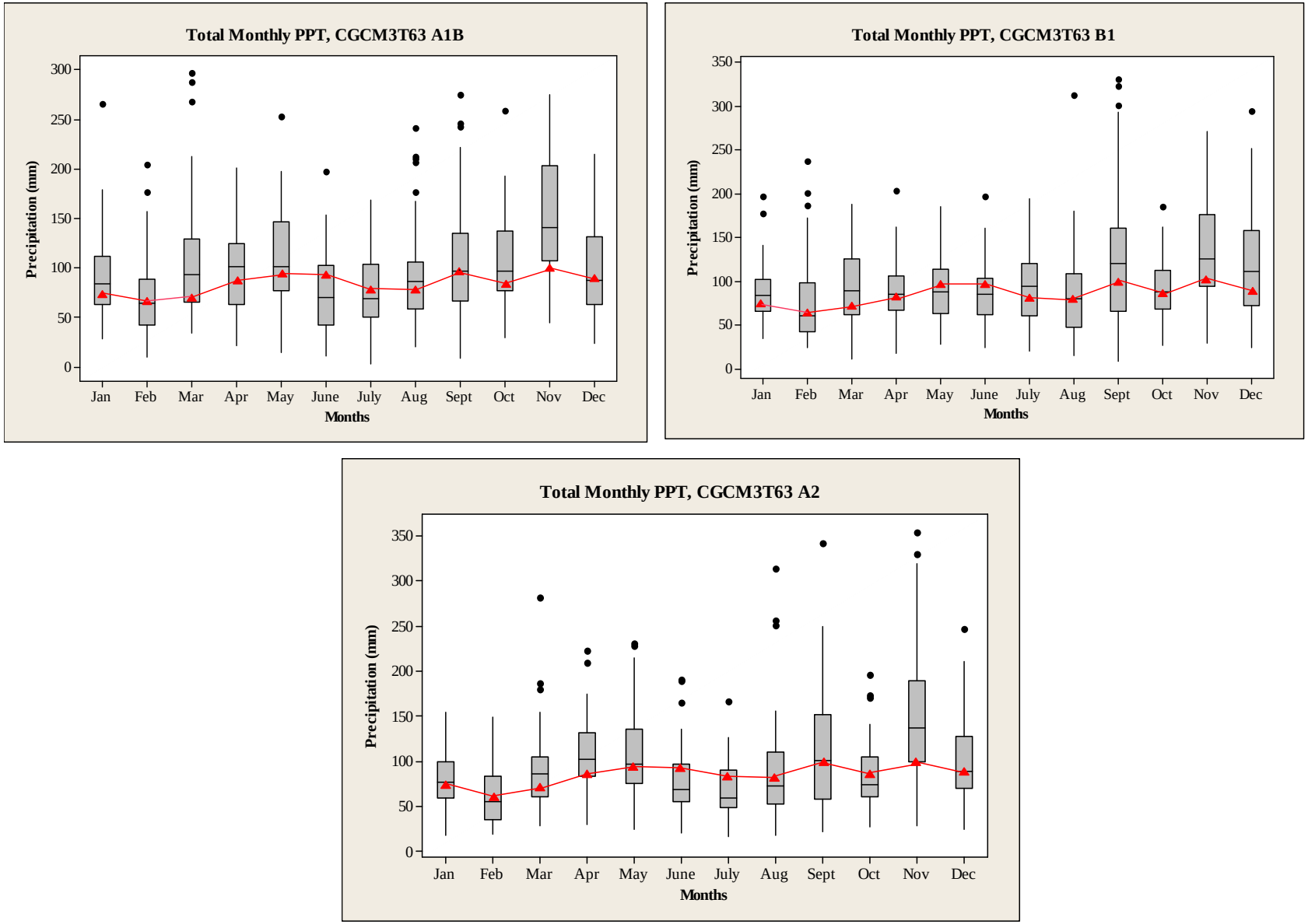

Figure 14: Box plots of CGCM3T63 generated monthly precipitation for A1B (upper left), A2 (upper right) and B1 scenarios

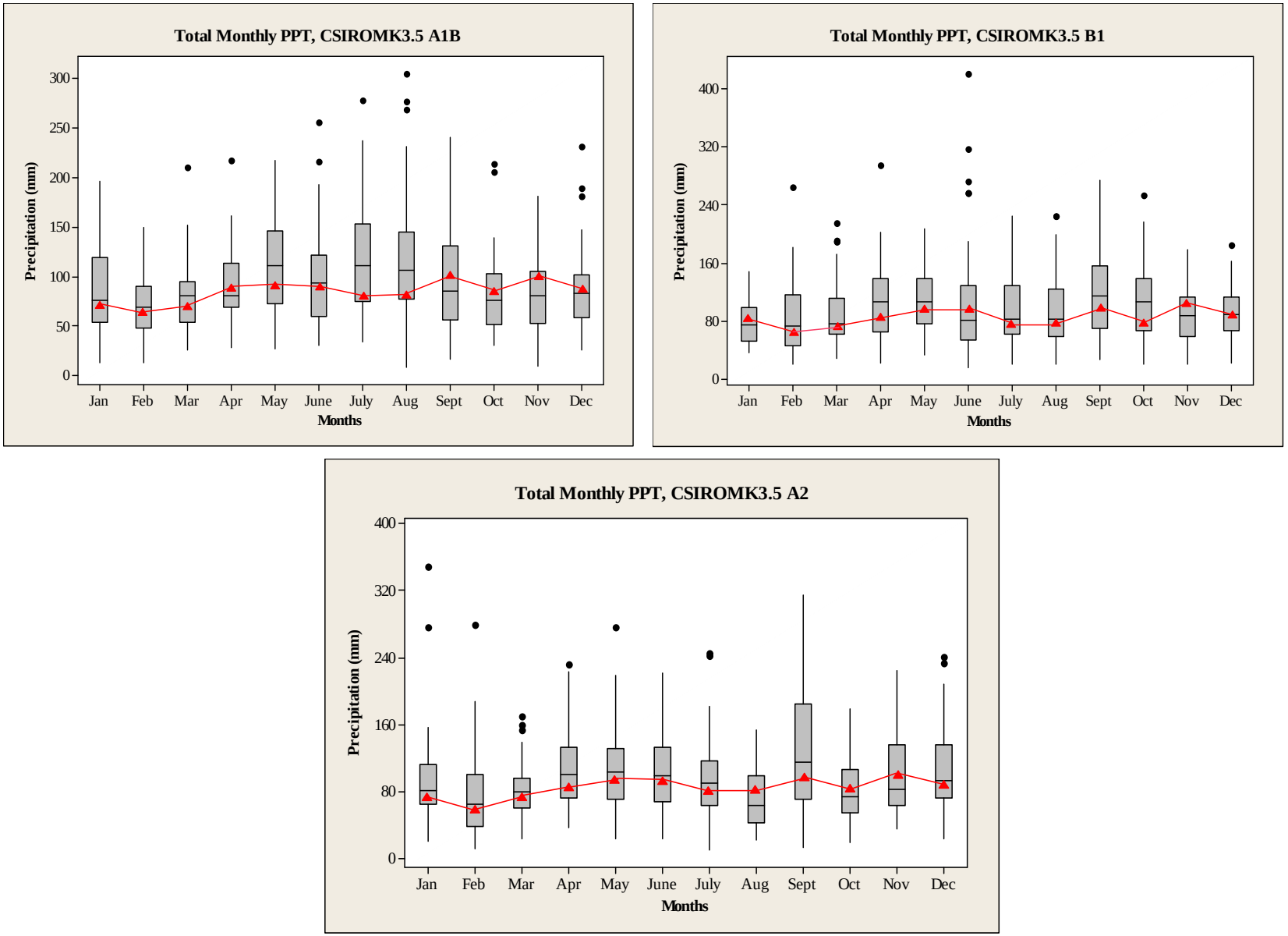

Figure 15: Box plots of CSIROMK3.5 generated monthly precipitation for A1B (upper left), A2 (upper right) and B1 scenarios

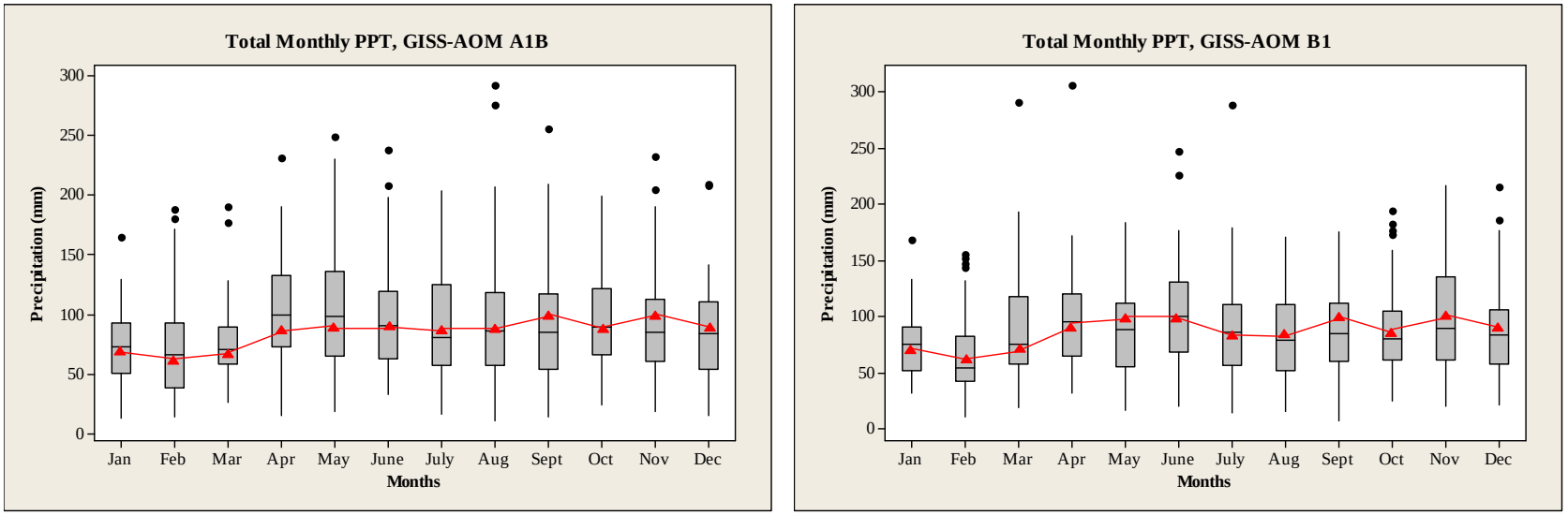

Figure 16: Box plots of GISS-AOM generated monthly precipitation for A1B (left), B1 (right) scenarios

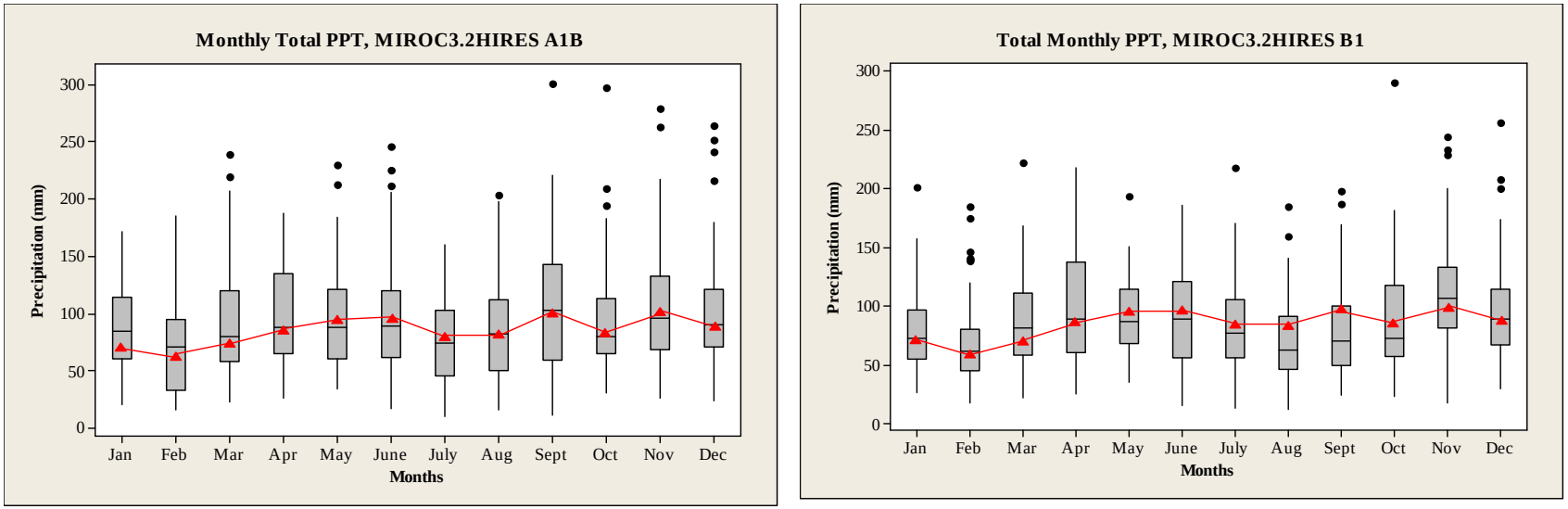

Figure 17: Box plots of MIROC3.2HIRES generated monthly precipitation for A1B (left), B1 (right) scenarios

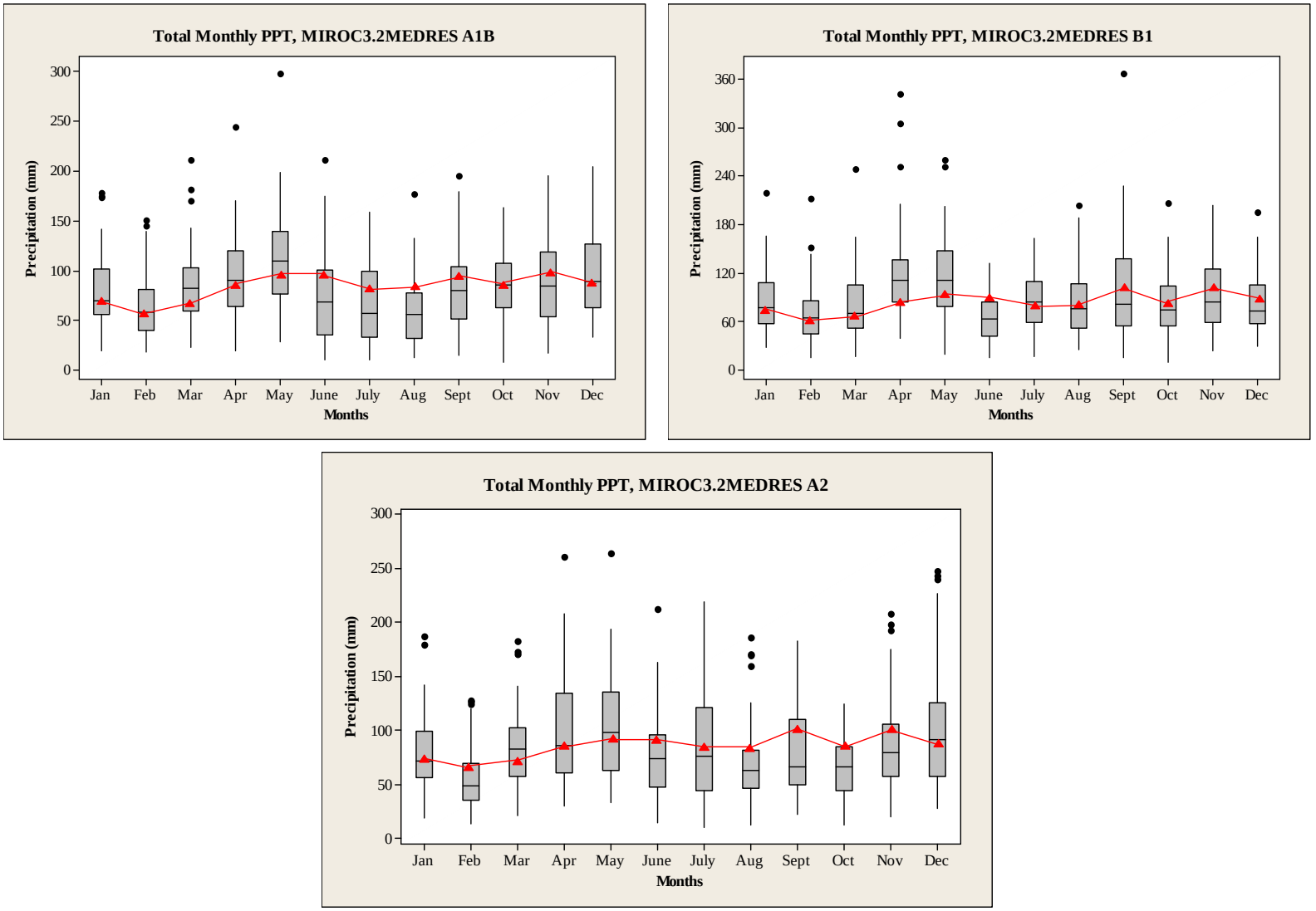

Figure 18: Box plots of MIROC3.2MEDRES generated monthly precipitation for A1B (upper left), A2 (upper right) and B1 Scenarios

5.4 Simulation of extreme events

A moderate change in precipitation can have large impact on the runoff, and thus on the occurrence of floods. The change is climate is predicted to shift the runoff pattern in Canada: reductions in spring and summer runoff, increase in winter runoff and earlier peak runoff (Sharif and Burn, 2007). It is therefore important to assess the changes in extreme precipitation amounts. In this study, three precipitation indices (Table 3), proposed by Vincent and Mekis (2006) have been used for comparing the performances of the AOGCMs in generating heavy precipitation amounts.

Table 3: List of Extreme Precipitation Indices

Precipitation Indices	**Definitions**	**Units**
Heavy precipitation days (>= 10 days)	Number of days with precipitation >= 10 mm	days
Very wet days (>= 95^{th} percentile)	Number of days with precipitation >=95^{th} percentile	days
Highest 5-day precipitation amount	Maximum precipitation sum for 5 day interval	mm

These indices demonstrate precipitation frequency, intensity and extremes. The highest 5 day precipitation, very wet days and the heavy precipitation days express extreme features of precipitation. For very wet days, the 95^{th} percentile reference value (18.3 mm) has been obtained from all non-zero total precipitation events for 1979-2005. It is better to use indices based on percentile values rather than a fixed threshold in Canada due to large variations of precipitation intensities in various regions.

Table 4: Change in Precipitation Indices Compared to 1979-2005

Scenarios	No. of Heavy prec. days	No. of very wet days	5 day-max. Precipitation, mm
CGCM3T47_A1B	0.963	0.500	-0.771
CGCM3T47_A2	2.759	2.537	5.738
CGCM3T47_B1	-2.370	-1.389	-4.351
CGCM3T63_A1B	3.037	2.074	4.765
CGCM3T63_A2	-2.389	-1.370	3.592
CGCM3T63_B1	1.481	1.130	-1.979
CSIROMK3.5_A1B	-1.963	-2.278	1.359
CSIROMK3.5_A2	2.463	1.778	8.432
CSIROMK3.5_B1	-0.704	0.481	-0.236
GISS-AOM_A1B	-1.778	-2.093	-18.066
GISS-AOM_B1	-2.296	-1.778	-4.286
MIROC3.2HIRES_A1B	2.519	2.407	12.595
MIROC3.2HIRES_B1	-0.685	-1.148	-12.762
MIROC3.2MEDRES_A1B	-2.296	-2.204	-1.534
MIROC3.2MEDRES_A2	-0.648	-0.019	0.513
MIROC3.2MEDRES_B1	2.000	1.593	14.542

Figure 19 and Appendix C presents probability plots of heavy precipitations generated by the AOGCMs at 95% confidence interval (upper and lower bound in each set) with Weibull distribution using Maximum Likelihood estimates. The parameter estimates have been displayed with Anderson-Darling (AD) goodness-of-fit statistic and associated p value. The AD measure how well several distributions from several AOGCMs follow the historic observation. A lower value of p (usually <0.05) indicates the data do not follow the specified distribution. For comparison of several distributions with AD, the smallest AD statistic indicates the closest fit to the data. One common feature of all AOGCMs are that they are positively (rightward) skewed indicating more data points in the right tail in the upper half than expected. This clearly suggests increase in the number of heavy precipitation days. The higher AD and lower p (<0.5) values

indicate that the CGCM3T47 A1B, CGCM3T63 A1B, MIROC3.2MEDRES A1B and B1 scenarios does not follow the same data distribution as the historic one. Changes in the precipitation indices compared to the historic observed 1979-2005 values are computed and presented in Table 4. The mean change in the heavy precipitation is not very significant over 54 year period; CGCM3T63 A1B shows an increase of 3 days of heavy precipitation events. Interestingly, a few models have shown a decrease in the occurrences of heavy precipitation days. So the deviation of the occurrence of heavy precipitation days between the AOGCMs is 5.3 days.

Figure 20 and Appendix D shows comparison plots of the frequency of occurrence as predicted by AOGCMs. CGCM3T47 A2, CSIROMK3.5 A2, CGCM3T63 A1B scenarios have predicted higher occurrence of very wet days with an increase of 2.5 days. However, scenarios, such as MIROC3.2MEDRES A1B, GISS-AOM B1 and CSIROMK3.5 A1B scenarios have predicted decrease of 2 very wet days. So in this case also, the differences between the AOGCMs are 5 days (Table 4).

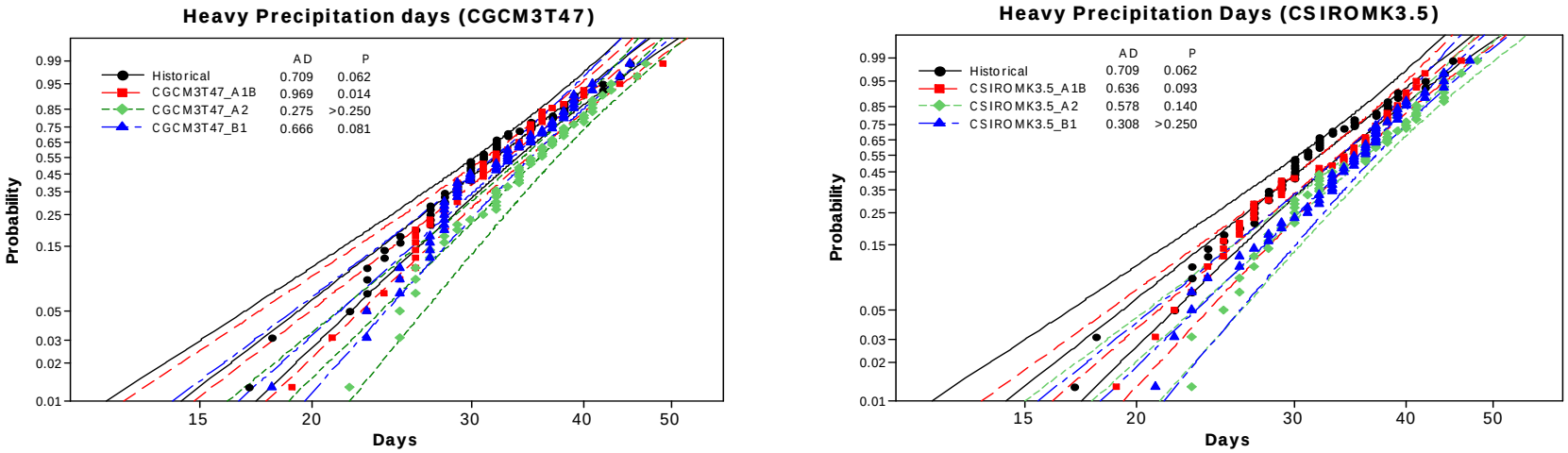

Figure 19: Probability plot of heavy precipitation days with > 10 mm precipitation generated by (a) CGCM3T47 (left) and (b) CSIROMK3.5 (right)

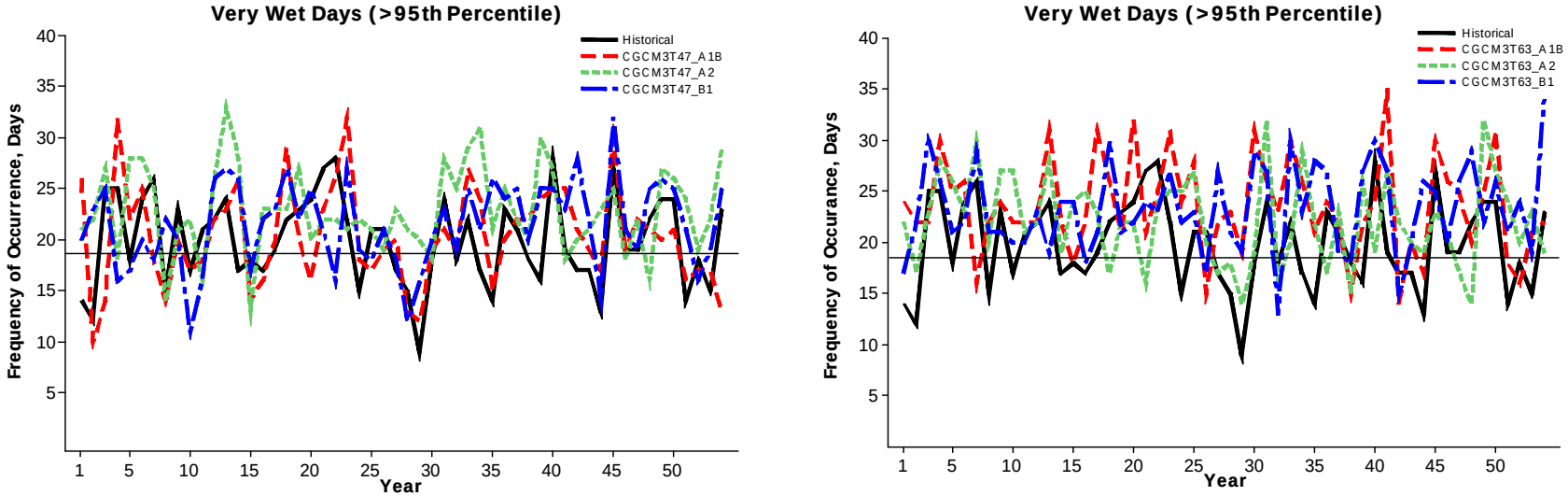

Figure 20: Time series plot of very wet days with > 95th percentile precipitation

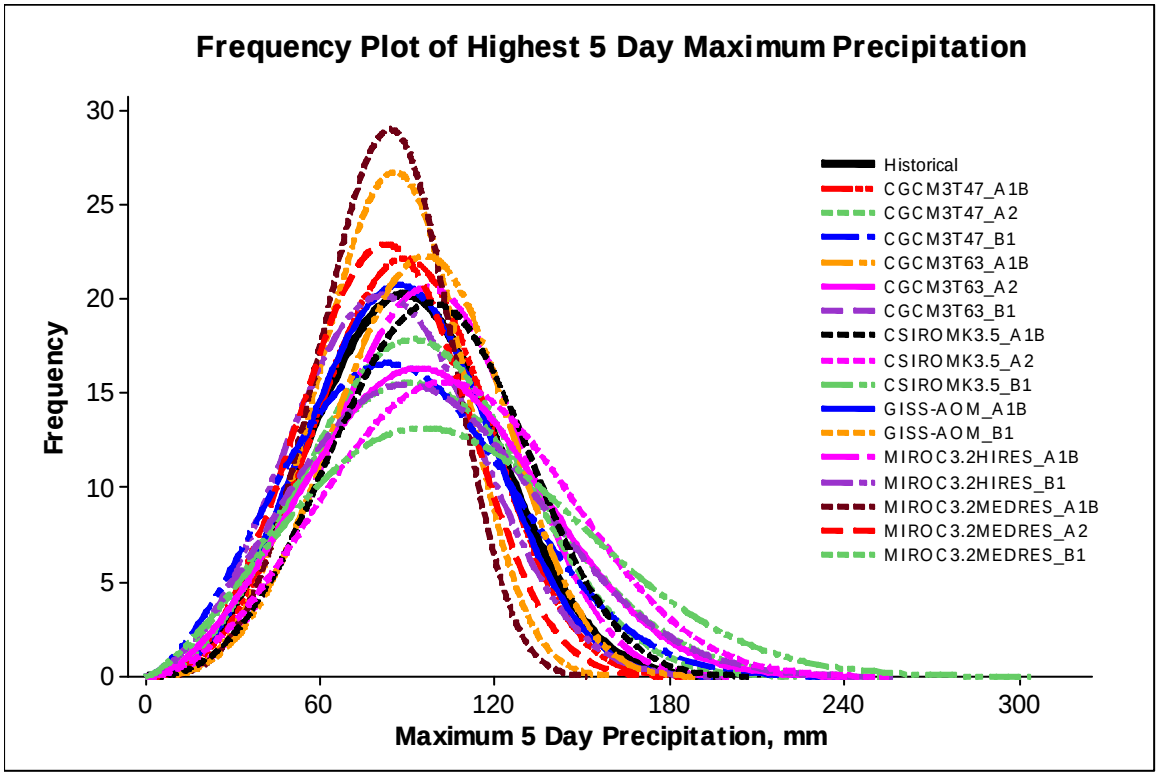

Figure 21: Frequency plot of maximum 5 day precipitation

Figure 21 presents frequency plot of highest 5 day maximum precipitation, accumulated over each year. The AOGCMs have predicted a wide variation in predicting the extent of the precipitation amounts. From the relative position of the peaks of GISS-AOM B1, CGCM3T47 A1B shows that these models have captured the highest 5 day precipitations very well. The shorter and wider-looking fitted distributions of CGCM3T47 A2 and CGCM3T63 B1 have shown greater variability. However, the highest frequency of the 5 day maximum precipitation ranges between 60-120 mm for most of the scenarios. The change in the precipitation amounts, however, does not show any specific pattern (Table 4).

6. Conclusions and Recommendations

This study investigates the potential impact of climate change on the Upper Thames River Basin using Principal component analysis integrated weather generator algorithm. Six AOGCM models have been used along with three SRES emissions scenarios. 54 years of synthetic data has been created using the WG-PCA algorithm with downscaled AOGCM data. For the purpose of comparing performances of AOGCM's WG results for London station has been chosen. The weather generator has been able to adequately reproduce a historic dataset which is statistically similar to the observed data. The model has also been able to simulate future plausible scenarios presented by the AOGCMs. For a given scenario this model has produced an unprecedented amount of precipitations, thus enabling higher accuracy of generating higher and lower extreme values which is more appropriate of assessing the flood and draught conditions in the study area under a changed climate. Generated results have been able to keep the correlation structure of the observed values which is important to produce hydrologic models at watershed scale. The climate change scenario simulations indicate wider variability in between the plausible scenarios. Overall, all models have indicated increase in maximum temperature, ranging from 1.5-6^0 C and a decrease in summer precipitation and increase in wintertime precipitation. The performances of the AOGCMs in predicting extreme precipitation indices are assessed by precipitation indices. No consistent pattern has been found in the number of highest 5 day maximum precipitations. The variabilities between the AOGCMs are even wider in case of extreme precipitation, which increases the difficulty of detecting a significant pattern. Overall, the above results have improved the present understanding of daily and extreme precipitation events in the study area. This

inconsistency clearly indicates the need for regional studies to explore local characteristics of precipitation extremes and improving the model quality by introducing more input variables relevant to the precipitation extremes.

Acknowledgement

The research presented in this study is funded by the Canadian Foundation for Climatic and Atmospheric Sciences.

REFERENCES

Allan, R. P., Soden, B. J. (2008) "Atmospheric Warming and the Amplification of Precipitation Extremes" *Science* 321: 1480-1484.

Barnett, D. N., Brown, S. J., Murphy, J. M., Sexton, D. M. H., Webb, M. J. (2006). "Quantifying uncertainty in changes in extreme event frequency in response to doubles CO2 using a large ensemble of GCM simulations." *Climate Dynamics* 26(5): 489-511. doi:10.1007/s00382-005-0097-1.

Canadian Climate Change Scenarios Network. "Main Issues and Criteria" *Environment Canada.* Retrieved August 19, 2009 from http://www.cccsn.ca/Scenarios/Main_Issues-e.html

Carter, T. R., Parry, M. L., Harasawa, H. and Nishioka, S. (1994). IPCC technical guidelines for assessing climate change impacts and adaptations, University College, London, United Kingdom, and Centre for Global Environmental Research, Tsukuba, Japan.

Chen, C-T., Knutson, T. (2008). “Notes and Correspondence On the Verification and Comparison of Extreme Rainfall Indices from Climate Models” *Journal of Climate* 21:1605-1621.

Choi, W., Moore, A., Rasmussen, P. F. (n. d.) “Simulating streamflow response to climate scenarios in central Canada using a simple statistical downscaling method incorporating changed variability”. doi: 10.3354/cr00826.

Diaz-Neito, J., Wilby, R. L. (2005). “A comparison of statistical downscaling and climate change factor methods: Impacts on low flows in the River Thames, United Kingdom”. *Climatic Change* 69: 245-268.

Dibike, Y. B., Gachon, P., St-Hilaire, A., Ouarda T. B. M. J., Nguyen, Van T-V. (2008) “Uncertainty analysis of statistically downscaled temperature and precipitation regimes in Northern Canada” *Theoretical and Applied Climatology* 91: 149-170.

Druyan, L. M., Fulakeza, M. and Lonergan, P. (2002). “Dynamic downscaling of seasonal climate predictions over Brazil”. *J Climate*, 15 (23), 3411-3426.

Eum, H-I., Arunachalam V., Simonovic, S.P. (2009) “Integrated Reservoir Management System for Adaptation to Climate Change Impacts in the Upper Thames River Basin” *Water Resources Research Report 62*, Facility for Intelligent Decision Support, Department of Civil and Environmental Engineering, London, Ontario, Canada.

Fowler, H. J., Ekstrom, M. and Kilsby, C. G. (2005). “New estimates of future changes in extreme rainfall across the UK using regional climate model integrations 1. Assessment of control climate”. *J Hydrol*, 300 (1-4), 212-233.

Flato, G. M.. "The Third Generation Coupled Global Climate Model (2005)". *Canadian*

Centre for Climate Modelling and Analysis. Environment Canada. Retrieved 23 Aug 2009 http://www.cccma.bc.ec.gc.ca/models/cgcm3.shtml.

Furrer, E. M. and Katz, R. W.(2008). "Improving the simulation of extreme precipitation events by stochastic weather generators". Water Resources Research, 44, W12439, doi: 10.1029/2008WR007316.

Giorgi, F. (1990). "Simulation of regional climate using a limited area model nested in a general-circulation model". *J Climate*, 3 (9), 941-963.

Giorgi, F., Marinucci, M. R. and G. A. Visconti (1992). "2 x CO2 climate change scenario over Europe generated using a limited area model nested in a general-circulation model.2. climate change scenario, *J Geophys Res-Atmos*, 97 (D9), 10011-10028.

Ghosh, S. (2007). "Hydrologic impacts of climate change: uncertainty modeling." *PhD thesis*, Department of Civil Engineering, Indian Institute of Science, Bangalore, India.

Hughes, J. P. (1993). "A Class of Stochastic Models for Relating Synoptic AtmosphericPatterns to Local Hydrologic Phenomena". *Ph.D. thesis*, University of Washington, US.

Hughes, J. P., and Guttorp, P. (1994). "A class of stochastic models for relating synoptic atmospheric patterns to regional hydrologic phenomena". *Water Resources Research*, 30 (5), 1535-1546.

Hughes, J. P., Guttorp, P. and Charles, S. P. (1999). "A non-homogeneous hidden markov model for precipitation occurrence". *Appl. Statist.*, 48 (1), 15-30.

IPCC, (2007). Climate Change 2007: The Physical Science Basis. Contribution of Working Group I to the Fourth Assessment Report of the Intergovernmental Panel on Climate Change [Solomon, S., D. Qin, M. Manning, Z. Chen, M. Marquis, K.B. Averyt, M. Tignor and H.L. Miller (eds.)]. Cambridge University Press, Cambridge, United Kingdom and New York, NY, USA, 996 pp.

Kilsby, C. G., Jones P. D., Burton, A., Ford, A. C., Fowler, H. J., Harpham, C., James, P., Smith, A., Wilby, R. L. (2007) "A Daily weather generator for use in climate change studies" *Environmental Modelling and Software* 22:1705-1719.

Koutsoyiannis, D., (2004). "Statistics of extremes and estimation of extreme rainfall, 1, Theoretical investigation". *Hydrological Sciences Journal*, 49 (4), 575–590.

Labat, D., Godderis, Y., and Probst, J. L. (2004) "Evidence for global runoff increase related to climate warming", *Advances in Water Resources*, 27: 631–642.

Magnuson, J.J., Robertson, D.M., Benson, B.J., Wynne, R.H., Livingstone, D.M., Arai, T., Assel, R.A., Barry, R.G., Card, V., Kuusisto, E., Granin, N.C., Prowse, T.D., Stewart, K.M. and Vuglinski, V.S., (2000). "Historic trends in lake and river ice cover in the Northern Hemisphere". *Science*, 289, 1743-1746.

Nakicenovic, N., Alcamo, J., Davis, G., de Vries, B., Fenhann, J., and co-authors (2000) "IPCC Special Report on Emissions Scenarios." *UNEP/GRID-Ardenal Publications*.

PCMDI (2005) "Model Information of Potential Use to the IPCC Lead Authors and the AR4: GISS-AOM." *CMIP3 Climate Model Documentation, References, and Links*. Retrieved 23 Aug 2009 from http://www-pcmdi.llnl.gov/ipcc/model_documentation/GISS-AOM.htm.

Prodanovic, P., and Simonovic, S. P. (2006). “Inverse Flood Risk Modelling of The Upper Thames River Basin”, *Water Resources Research Report* no. 052, Facility for Intelligent Decision Support, Department of Civil and Environmental Engineering, London, Ontario, Canada.

Prodanovic, P., Simonovic, S. P. (2007). “Development of rainfall intensity duration frequency curves for the City of London under the changing climate”, *Water Resources Research Report* no. 58, Facility for Intelligent Decision Support, Department of Civil and Environmental Engineering, London, Ontario, Canada.

Schimidli, J., Frei, C. and Vidale, P. L. (2006). Downscaling from GCM precipitation: A benchmark for dynamical and statistical downscaling methods. *International Journal of Climatology*, 26, 679-689.

Semenov, M. A., Barrow E. M. (1997). “Use of a stochastic weather generator in the development of climate change scenarios” *Climatic Change*, 35:397-414.

Sharif, M. and Burn, D. H. (2007). “Improved K-nearest neighbor weather generating model. *Journal of Hydrologic Engineering*, American Society of Civil Engineers. DOI: 10.1061/(ASCE)1084-0699 (2007)12:1(42).

Sharif, M, and Burn, D. (2006). "Simulating climate change scenarios using an improved K-nearest neighbor model’, Jo*urnal of hydrology*, (325), 179-196.

Vidal, J-P., Wade, S. (2008) “A framework for developing high-resolution multi-model climate projections: 21st century scenarios for the UK” *International Journal of Climatology* 28: 843-858.

Vincent, L. and Mekis, E., (2006). “Changes in daily and extreme temperature and precipitation indices for Canada over the twentieth century”. *Atmosphere-Ocean*, 44, 177-193.

Walsh, K. and J. L. Mcgregor, Jl. (1995). “January and July climate simulations over the Australian region using a limited-area model”. *J Climate*, 8 (10), 2387-2403.

Wheaton, E., Wittrock, V., Kulshretha, S., Koshida, G., Grant, C., Chipanshi, A. and Bonsal, B., 2005. Lessons Learned from the Canadian Drought Years of 2001 and 2002. *Synthesis Report, Saskatchewan Research Council* Publication No. 11602-46E03, Saskatoon, Saskatchewan, 38 p.

Whitfield, P.H. and Cannon, A.J., (2000). “Recent variations in climate and hydrology in Canada”. *Canadian Water Resources Journal*, 25(1), 19-65.

Wigley, T. L., Jones, P. D., Briffa, K. R., and Smith, G. (1990). “Obtaining sub-grid-scale information from coarse-resolution general circulation model output”. *J. Geophys. Res.*, 95 (D2), 1943-1953.

Wilby, R.L. and Wigley, T.M.L. (1997). “Downscaling general circulation model output: a review of methods and limitations”. *Progress in Physical Geography* **21**, 530-548.

Wilcox, E. M., Donner, L. J. (2007).“The frequency of extreme rain events in satellite rain-rate estimates and an atmospheric general circulation model” *Journal of Climate* 20(1): 53-69.

Wilks, D. S. and Wilby, R. L. (1999). “The weather generation game: a review of stochastic weather models”. *Progress in Physical Geography*, 23 (3), 329-357.

Yates, D., Gangopadhyay, S., Rajagopalan, B., and Strzepek, K. (2003). “A technique for generating regional climate scenarios using a nearest-neighbor algorithm”. *Water Resources Research, 39*(7), 1199-1213

Zhang, Q., Xu, C-Y., Zhang, Z., Chen, Y. D., Liu, C-L., and Lin, H. (2008). “Spatial and temporal variability of precipitation maxima during 1960 – 2005 in the Yangtze River basin and possible association with large scale circulation”. *Journal of Hydrology*, 353: 215–217. doi:10.1016/j.jhydrol.2007.11.023

Zhang, X., Harvey, K., Hogg, W. and Yuzyk, T., (2001). “Trends in Canadian streamflow”. *Water Resources Research*, 37, 987-998.

APPENDIX A

SRES Scenarios

Figure A1: SRES Emission Scenarios (Nakicenovic et al, 2000)

A1B: In scenario A1B, the storyline includes rapid economic expansion and globalization, a population peaking at 9 billion in 2050, and a balanced emphasis on a wide range of energy sources (Nakicenovic et al, 2000).

B1: The storyline for the B1 scenario is much like A1B in terms of population and globalization; however there are changes toward a service and information economy with more resource efficient and clean technologies. Emphasis is put on finding global solutions for sustainability (Nakicenovic et al, 2000).

A2: In A2, the storyline consists of a world of independently operating nations with a constantly increasing population and economic development on a regional level. Technological advances in this storyline occur more slowly due to the divisions between nations (Nakicenovic et al, 2000).

APPENDIX B

Atmosphere-Ocean General Circulation Model data description

Canadian Coupled Global Climate Model

The third generation Coupled Global Climate Model (CGCM3) was created in 2005 by the Canadian Centre for Climate Modelling and Analysis (CCCma) in Victoria, BC for use in the IPCC 4th assessment report to run complex mathematical equations which describe the earth's atmospheric and oceanic processes. The CGCM3 climate model includes four major components: an atmospheric general circulation model, an ocean general circulation model, a thermodynamic sea-ice model, and a land surface model (Hengeveld, 2000) and consists of two resolutions, T47 and T63. CGCM3T47 has a spatial resolution of 3.75° x 3.75° and it includes 31 vertical levels (Flato, 2005). The atmospheric resolution of CGCM3T63 model is 2.8° × 2.8°. The emissions scenarios A1B, A2 and B1 were used as greenhouse gas inputs in both models.

Commonwealth Scientific and Industrial Research Organization's Mk3.5 Climate Systems Model

Australia's Commonwealth Scientific and Industrial Research Organization created the AOGCM CSIROMK3.5, which is an improved version of the MK climate systems model. The spatial resolution of the model is 1.875 × 1.875. The SRES emissions scenarios A1B, A2, and B1 were used as inputs to the model for the IPCC 4th assessment report.

Goddard Institute for Space Studies' Atmospheric Ocean Model

The North American Space Association and the Goddard Institute for Space Studies developed the GISS-AOM climate model, first in 1995 and then a revised version was created with smaller grids in 2004 for the IPCC 4th assessment report. The resolution for the model is 4° longitude by 3° latitude (PCMDI, 2005). The atmospheric grid has 12 vertical layers (PCMDI, 2005). The emissions scenarios SRES A1B and B1 were used as greenhouse gas inputs to the model.

Model for Interdisciplinary Research on Climate version 3.2

The Japanese Model for Interdisciplinary Research on Climate version 3.2 (MIROC3.2) was developed in two resolutions: the high resolution (MIROC3.2HIRES) in 1.125° × 1.125° grid and the medium resolution (MIROC3.2MEDRES) in 2.8° × 2.8° grid. For present study, two emissions scenarios from MIROC3.2HIRES (A1B and B1) and three scenarios (A1B, A2 and B1) from MIROC3.2MEDRES were used.

APPENDIX C

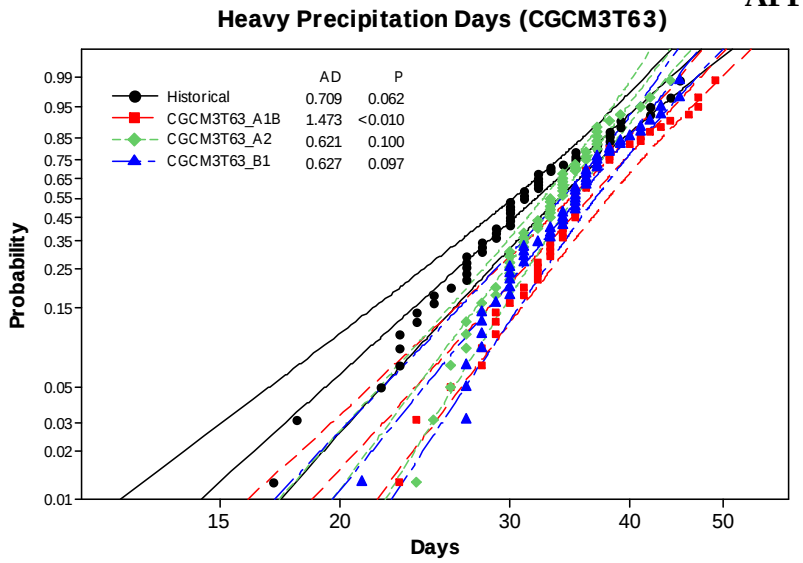
Heavy Precipitation Days (CGCM3T63)
AD P
Historical 0.709 0.062
CGCM3T63_A1B 1.473 <0.010
CGCM3T63_A2 0.621 0.100
CGCM3T63_B1 0.627 0.097
Probability
Days

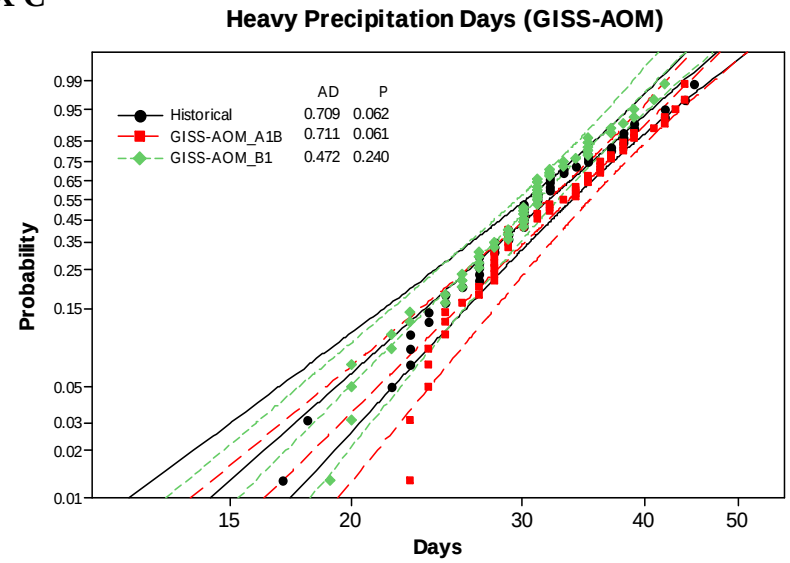
Heavy Precipitation Days (GISS-AOM)
AD P
Historical 0.709 0.062
GISS-AOM_A1B 0.711 0.061
GISS-AOM_B1 0.472 0.240
Probability
Days

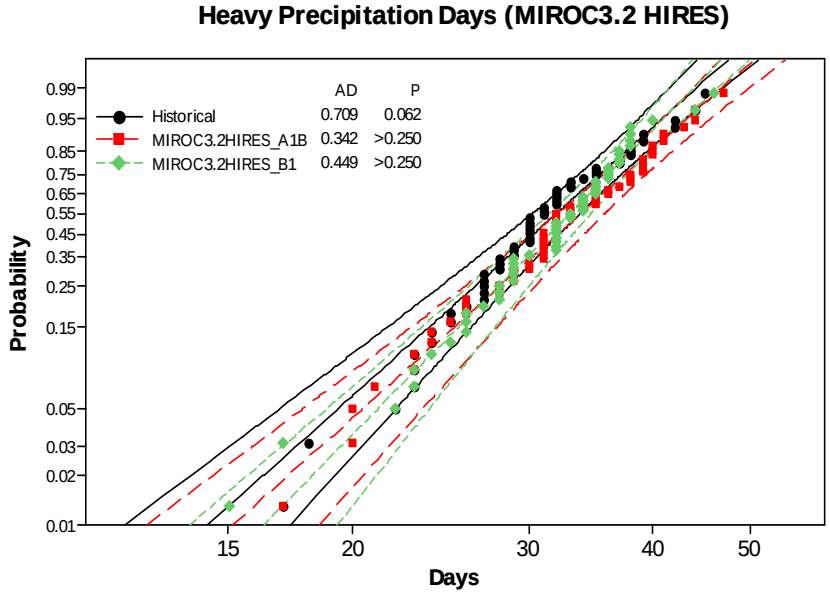
Heavy Precipitation Days (MIROC3.2 HIRES)
AD P
Historical 0.709 0.062
MIROC3.2HIRES_A1B 0.342 >0.250
MIROC3.2HIRES_B1 0.449 >0.250
Probability
Days

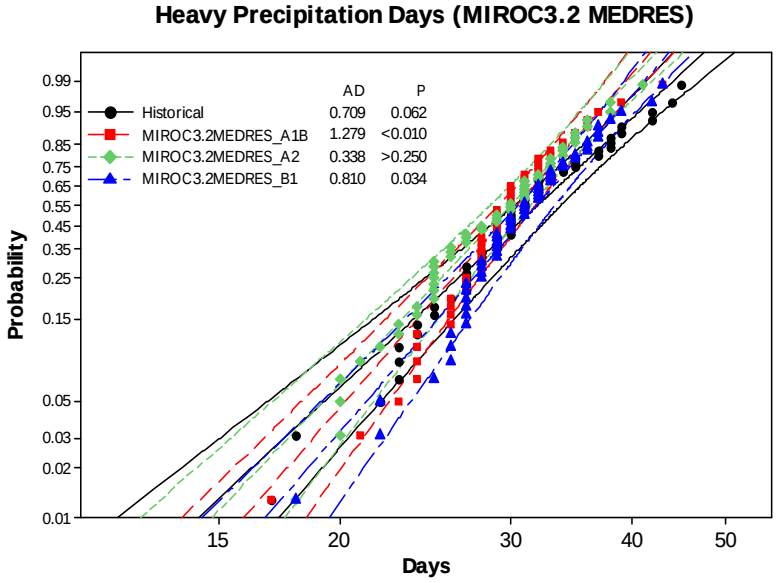
Heavy Precipitation Days (MIROC3.2 MEDRES)
AD P
Historical 0.709 0.062
MIROC3.2MEDRES_A1B 1.279 <0.010
MIROC3.2MEDRES_A2 0.338 >0.250
MIROC3.2MEDRES_B1 0.810 0.034
Probability
Days

APPENDIX D

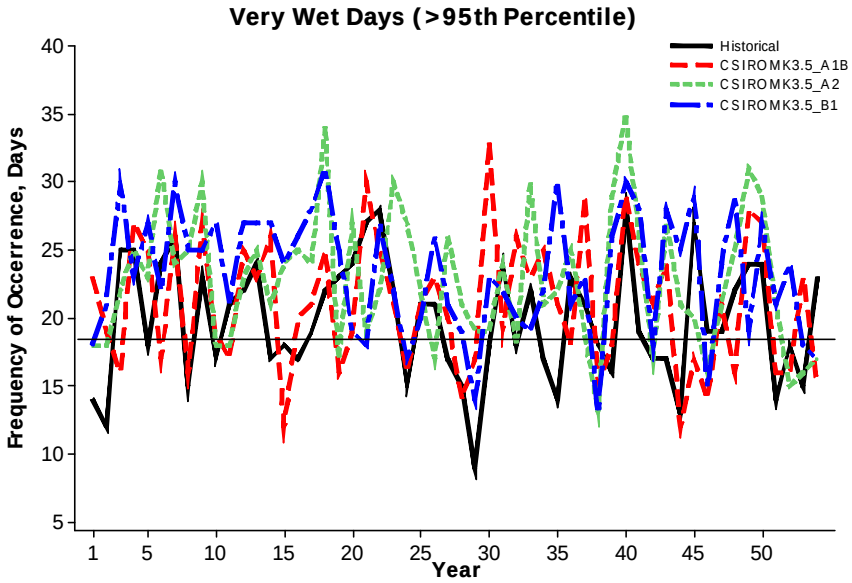
Very Wet Days (>95th Percentile)
Historical
CSIROMK3.5_A1B
CSIROMK3.5_A2
CSIROMK3.5_B1
Frequency of Occerrence, Days
Year

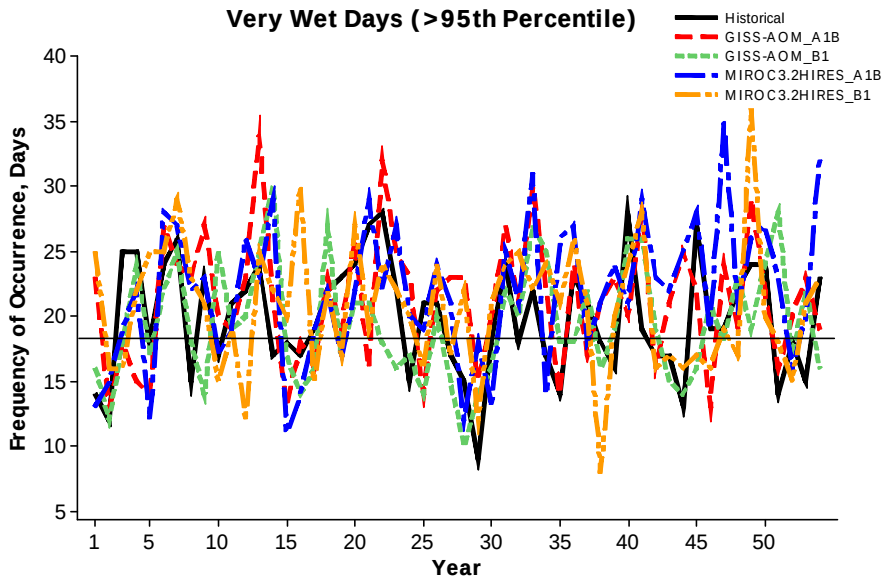
Very Wet Days (>95th Percentile)
Historical
GISS-AOM_A1B
GISS-AOM_B1
MIROC3.2HIRES_A1B
MIROC3.2HIRES_B1
Frequency of Occurrence, Days
Year

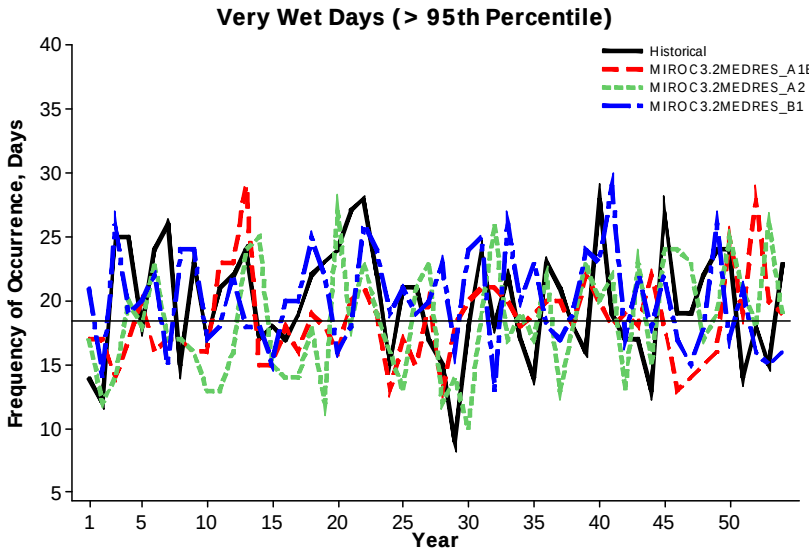
Very Wet Days (> 95th Percentile)
Historical
MIROC3.2MEDRES_A1B
MIROC3.2MEDRES_A2
MIROC3.2MEDRES_B1
Frequency of Occurrence, Days
Year